RNA helicase activity to unwind the double-stranded RNA during the synthesis of genomic RNA [5,6].

Although the previous standard therapy, combining pegylated interferon with ribavirin, was effective in only about half of patients infected with genotype 1, the most common genotype worldwide [7–9], recent biotechnological advances have led to the development of a novel therapy using anti-HCV agents that directly target HCV proteins or host factors required for HCV replication and have improved the sustained virologic response (SVR) [10–12]. Telaprevir and boceprevir, which are categorized as advanced NS3/4A protease inhibitors, were recently approved for the treatment of chronic hepatitis C patients infected with genotype 1 [13,14]. The triple combination therapy with pegylated interferon, ribavirin, and telaprevir improved SVR by 77% in patients infected with genotype 1 [15]. However, this therapy exhibits side effects including rash, severe cutaneous eruption, influenza-like symptoms, cytopenias, depression, and anemia [7,16,17]. Furthermore, the possibility of the emergence of drug-resistant viruses is a serious problem with therapies that use antiviral compounds [18,19].

Recent technical advances in the determination of molecular structures and the synthesis of chemical compounds have led to the development of various drugs based on natural products, especially drugs identified from terrestrial plants and microbes [20–22]. Marine organisms, including plants and animals, were recently established as representative of a natural resource library for drug development. Potent biological activity is often found in products isolated from marine organisms because of their novel molecular structures [23,24]. Trabectedin (Yondelis), cytarabine (Ara-C), and eribulin (Halaven), which are known as antitumor drugs, were developed from compounds found in marine organisms [25].

In this study, we screened 84 extracts prepared from 54 marine organisms by using replicon cell lines derived from HCV genotype 1b and attempted to identify the extract that inhibits HCV RNA replication. A marine organism may produce anti-HCV agent(s) that could inhibit the protease and helicase activities of NS3.

Results

Effect of the Extract from Marine Sponge and Tunicate on HCV Replication

We prepared methanol (MeOH)- and ethyl acetate (EtOAc)-soluble extracts from 54 marine organisms in order to test which of these extracts could best suppress HCV replication. Each extract was added at 25 μg/ml to the culture supernatant of HCV replicon cell lines derived from O and Con1 strains of genotype 1b, which produce the luciferase/neomycin hybrid protein depending on RNA replication. Luciferase activity and cell viability were measured 72 h after treatment with the extracts (Table 1). The extracts exhibiting more than 85% cell viability and lower than 15% luciferase activity were selected as arbitrary candidates for the extract including anti-HCV compounds. The EtOAc-extract prepared from sample C-29 (C-29EA) was selected as a candidate in both cell lines. Thus, the anti-HCV activity of extract C-29EA was tested.

The EtOAc-soluble extract C-29EA was prepared from the marine sponge *Amphimedon* sp. (Fig. 1A), which inhabits the sea surrounding Okinawa Prefecture, Japan. HCV replication was inhibited in a dose-dependent manner but did not exhibit cytotoxicity when replicon cells were treated with C-29EA (Fig. 1 B). The extract C-29EA exhibited EC_{50} values of 1.5 μg/ml (Table 2). Furthermore, treatment with C-29EA suppressed the HCV replication derived from the genotype 2a strain JFH1 with an EC_{50} of 24.9 μg/ml, irrespective of cell viability (Fig. 2A and Table 2). Extract C-29EA also inhibited the production of infectious viral particles, viral RNA, and core protein from JFH1-infected cells in the supernatant (Fig. 2B and C). These results suggest that the marine sponge *Amphimedon* sp. possesses anti-HCV agents.

Effect of Extract C-29EA on IRES-dependent Translation

Extract C-29EA had the most potent inhibitory activity against HCV replication. The viral replication (Fig. 1 B and 2 A) and viral proteins (Fig. 3 A and B) in replicon cell lines derived from genotype 1b strain Con1 and 2a strain JFH1 were decreased 72 h after treatment in a dose-dependent manner. HCV protein has been translated based on the positive-sense viral RNA in an IRES-dependent manner. The replicon RNA of HCV is composed of the 5′-UTR of HCV, indicator genes (a luciferase-fused drug-resistant gene), encephalomyocarditis virus (EMCV) IRES, the viral genes encoding complete or nonstructural proteins, and the 3′-UTR of HCV, in that order [26]. The replicon RNA replicated autonomously in several HCV replication-permissive cell lines derived from several hepatoma cell lines. Nonstructural proteins in replicon cells were polycistronically translated through EMCV IRES. The cap-dependent translated mRNA, including *Renilla* luciferase, EMCV IRES, and the firefly luciferase/neomycin-resistant gene, in that order, was constructed to examine the effect of the extract on EMCV-IRES-dependent translation (Fig. 3C). When the mRNA expression was transcribed by an EF promoter of the transfected plasmid in the presence of C-29EA, the ratio of firefly luciferase activity to *Renilla* luciferase activity was not changed (Fig. 3C). This suggested that treatment with C-29EA exhibited no effect on EMCV-IRES-dependent translation. Furthermore, treatment with C-29EA did not significantly affect the activity of HCV IRES that was used instead of EMCV IRES in the system described above (Fig. 3D). Thus, these results suggest that treatment with C-29EA exhibits no effect on EMCV- or HCV-IRES-dependent translation.

Effect of C-29EA on the Interferon Signaling Pathway

It has been well known that HCV replication in cultured cells is potently inhibited by interferon [27,28]. We examined whether or not treatment with C-29EA elicits an interferon-inducible gene from replicon cells. The replicon cells were treated with various concentrations of interferon-alpha 2b or 15 μg of C-29EA per milliliter. The treated cells were harvested at 72 h post-treatment. The interferon-inducible gene 2′, 5′-OAS, was induced with IFN-alpha 2b but not with a 10-times EC_{50} concentration of C-29EA (Fig. 4). These results suggest that the inhibitory effect of C-29EA on the replication of the HCV replicon is independent of the IFN signaling pathway.

Effect of C-29EA on the NS3 Helicase Activity

We previously established an assay system for unwinding HCV activity based on photoinduced electron transfer (PET) [29,30]. The fluorescent dye (BODIPY FL) is attached to the cytosine at the 5′-end of the fluorescent strand and quenched by the guanine base at the 3′-end of the complementary strand via PET. When helicase unwinds the double-strand RNA substrate, the fluorescence of the dye emits a bright light upon the release of the dye from the guanine base. The capture strand, which is complementary to the complementary strand, prevents the reannealing of the unwound duplex. Treatment with C-29EA inhibited the helicase activity in a dose-dependent manner, with an IC_{50} value of 18.9 μg/ml (Fig. 5A). We confirmed the effect of C-29EA on NS3 helicase unwinding activity by the RNA helicase assay using ^{32}P-labeled double-stranded RNA (dsRNA) as a substrate. Treatment

Table 1. Effect of marine organism extracts on HCV replication and cell viability.

No.	Sample	Luciferase activity (% of control)		Cell viability (% of control)		Phylum	Specimen	Extract	Site
		O	Con1	O	Con1				
1	A-1	10	111	105	104	Sponge	*Unidentified*	MeOH	A
2	A-2	82	209	91	132	Soft coral	*Briareum*	MeOH	A
3	A-3	87	177	54	110	Tunicate	*unidentified*	MeOH	A
4	A-4	82	186	84	100	Sponge	*Liosina*	MeOH	A
5	B-5	110	165	86	110	Sponge	*unidentified*	MeOH	B
6	B-6	70	149	103	119	Sponge	*Xestospongia*	MeOH	B
7	B-7	89	191	111	144	Sponge	*Epipolasis*	MeOH	B
8	B-8	89	182	115	132	Sponge	*unidentified*	MeOH	B
9	B-9	57	72	92	124	Sponge	*Strongylophora*	MeOH	B
10	B-10	106	182	73	96	Sponge	*Stylotella aurantium*	MeOH	B
11	C-12	96	162	114	98	Sponge	*Epipolasis*	MeOH	B
12	C-13	123	141	91	103	Sponge	*unidentified*	MeOH	B
13	C-14	89	175	77	100	Sponge	*Hippospongia*	MeOH	B
14	C-16	80	177	108	88	Sponge	*unidentified*	MeOH	B
15	C-18	119	170	93	94	Sponge	*unidentified*	MeOH	B
16	C-19	0	0	0	4	Sponge	*unidentified*	MeOH	B
17	C-20	101	158	61	106	Sponge	*Xestospongia testudinaria*	MeOH	B
18	C-21	85	161	83	102	Sponge	*unidentified*	MeOH	B
19	C-22	109	88	38	89	Sponge	*unidentified*	MeOH	B
20	C-23	94	156	32	90	Sponge	*unidentified*	MeOH	B
21	C-24	118	86	42	94	Sponge	*Theonella*	MeOH	B
22	C-25	82	111	91	106	Sponge	*unidentified*	MeOH	B
23	C-27	0	0	15	2	Sponge	*unidentified*	MeOH	B
24	C-28	90	166	30	90	Sponge	*Petrosia*	MeOH	B
25	C-29	65	151	29	101	Sponge	*Amphimedon*	MeOH	B
26	D-31	81	127	55	91	Tunicate	*unidentified*	MeOH	C
27	D-32	80	141	47	93	Sponge	*unidentified*	MeOH	C
28	D-33	88	153	72	90	Gorgonian	*Junceella fragilis*	MeOH	C
29	E-35	114	156	40	118	Sponge	*Phyllospongia sp.*	MeOH	C
30	E-36	80	125	69	116	Tunicate	*Didemnum molle*	MeOH	C
31	E-37	88	129	54	108	Sponge	*Xestospongia sp.*	MeOH	C
32	E-38	70	153	35	112	Sponge	*unidentified*	MeOH	C
33	F-40	119	170	38	104	Sponge	*unidentified*	MeOH	C
34	F-41	88	166	48	101	Soft coral	*unidentified*	MeOH	C
35	G-42	113	157	31	126	Sponge	*unidentified*	MeOH	D
36	H-43	83	0	39	5	Sponge	*unidentified*	MeOH	D
37	J-44	62	183	27	105	Sponge	*Cinachyra*	MeOH	D
38	J-45	96	140	47	103	Sponge	*Liosina*	MeOH	D
39	J-46	83	149	77	102	Sponge	*unidentified*	MeOH	D
40	J-47	94	37	40	111	Sponge	*unidentified*	MeOH	D
41	J-48	24	16	53	70	Sponge	*Stylotella*	MeOH	D
42	J-49	78	123	55	105	Sponge	*unidentified*	MeOH	D
43	J-50	93	138	51	108	Sponge	*unidentified*	MeOH	D
44	J-51	103	73	41	115	Sponge	*unidentified*	MeOH	D
45	J-52	162	237	113	131	Sponge	*unidentified*	MeOH	D
46	J-53	51	90	93	122	Tunicate	*Didemnum*	MeOH	D
47	J-54	42	90	113	124	Sponge	*unidentified*	MeOH	D

Table 1. Cont.

No.	Sample	Luciferase activity (% of control)		Cell viability (% of control)		Phylum	Specimen	Extract	Site
		O	Con1	O	Con1				
48	J-55	88	133	131	110	Jellyfish	*unidentified*	MeOH	D
49	J-56	28	51	113	103	Sponge	*unidentified*	MeOH	D
50	J-57	8	63	94	85	Tunicate	*Pseudodistoma kanoko*	MeOH	D
51	J-58	0	2	48	65	Sponge	*unidentified*	MeOH	D
52	J-59	0	2	45	71	Sponge	*unidentified*	MeOH	D
53	J-60	98	134	122	95	Annelid	*unidentified*	MeOH	D
54	A-2	0	1	6	15	Soft coral	*Briareum*	EtOAc	A
55	A-3	0	0	6	9	Tunicate	*unidentified*	EtOAc	A
56	A-4	22	36	74	76	Sponge	*Liosina*	EtOAc	A
57	B-5	33	107	69	93	Sponge	*unidentified*	EtOAc	B
58	B-6	0	0	5	8	Sponge	*Xestospongia*	EtOAc	B
59	B-7	0	0	5	9	Sponge	*Epipolasis*	EtOAc	B
60	B-8	0	0	2	46	Sponge	*unidentified*	EtOAc	B
61	B-9	0	0	8	14	Sponge	*Strongylophora*	EtOAc	B
62	B-10	0	0	3	8	Sponge	*Stylotella aurantium*	EtOAc	B
63	C-12	0	0	4	14	Sponge	*Epipolasis*	EtOAc	B
64	C-13	0	0	4	5	Sponge	*unidentified*	EtOAc	B
65	C-14	48	119	82	102	Sponge	*Hippospongia*	EtOAc	B
66	C-15	0	0	8	11	Sponge	*unidentified*	EtOAc	B
67	C-18	0	0	4	3	Sponge	*unidentified*	EtOAc	B
68	C-19	23	76	63	109	Sponge	*unidentified*	EtOAc	B
69	C-20	34	32	63	112	Sponge	*Xestospongia testudinaria*	EtOAc	B
70	C-21	1	0	52	12	Sponge	*unidentified*	EtOAc	B
71	C-22	76	34	74	110	Sponge	*unidentified*	EtOAc	B
72	C-24	0	0	20	7	Sponge	*Theonella*	EtOAc	B
73	C-26	41	43	80	110	Sponge	*unidentified*	EtOAc	B
74	C-27	1	0	35	40	Sponge	*unidentified*	EtOAc	B
75	C-28	68	62	82	115	Sponge	*Petrosia*	EtOAc	B
76	C-29	10	11	93	88	Sponge	*Amphimedon*	EtOAc	B
77	D-31	20	71	85	120	Tunicate	*Eudistoma*	EtOAc	C
78	D-33	0	0	5	7	Gorgonian	*Junceella fragilis*	EtOAc	C
79	E-35	0	0	4	5	Sponge	*Phyllospongia sp.*	EtOAc	C
80	E-36	71	83	75	100	Tunicate	*Didemnum molle*	EtOAc	C
81	F-40	72	110	87	130	Sponge	*unidentified*	EtOAc	C
82	F-41	8	33	73	104	Soft coral	*unidentified*	EtOAc	C
83	H-43	0	197	4	119	Sponge	*unidentified*	EtOAc	D
84	J-46	113	58	103	126	Sponge	*unidentified*	EtOAc	D

There are a total of 54 marine organisms, while 84 extracts were prepared from them with ethyl acetate and/or methanol. Aragusuku, Iriomote, Kohama, and Ishigaki islands are indicated by A, B, C, and D, respectively, in the collection-site column?(right end). EtOAc: Ethyl acetate; MeOH: Methanol.

doi:10.1371/journal.pone.0048685.t001

with C-29EA inhibited dsRNA dissociation at a concentration of 16 μg/ml and above (Fig. 5B).

The unwinding ability of HCV helicase depends on ATP binding, ATP hydrolysis, and RNA binding [30,31]. We examined the effect of C-29EA on the ATPase activity of NS3. The ratio of free phosphate (^{32}P-Pi) to ATP (^{32}P-ATP) was determined in the presence of C-29EA. The reaction was carried out between 16 and 250 μg of C-29EA per milliliter. The ATPase activity of NS3 helicase was not inhibited (Fig. 6A), although the helicase activity was decreased to less than 20% in the presence of 50 μg of C-29EA per milliliter (Fig. 5A). Next, we examined the effect of C-29EA on the binding of NS3 helicase to single-strand RNA (ssRNA). A gel-mobility shift assay was employed to estimate the binding activity of NS3 to the 21-mer of ssRNA. The binding of NS3 to ssRNA was inhibited by C-29EA in a dose-dependent manner (Fig. 6 B and C). These results suggest that treatment with C-29EA inhibits the helicase activity of NS3 by suppressing RNA binding.

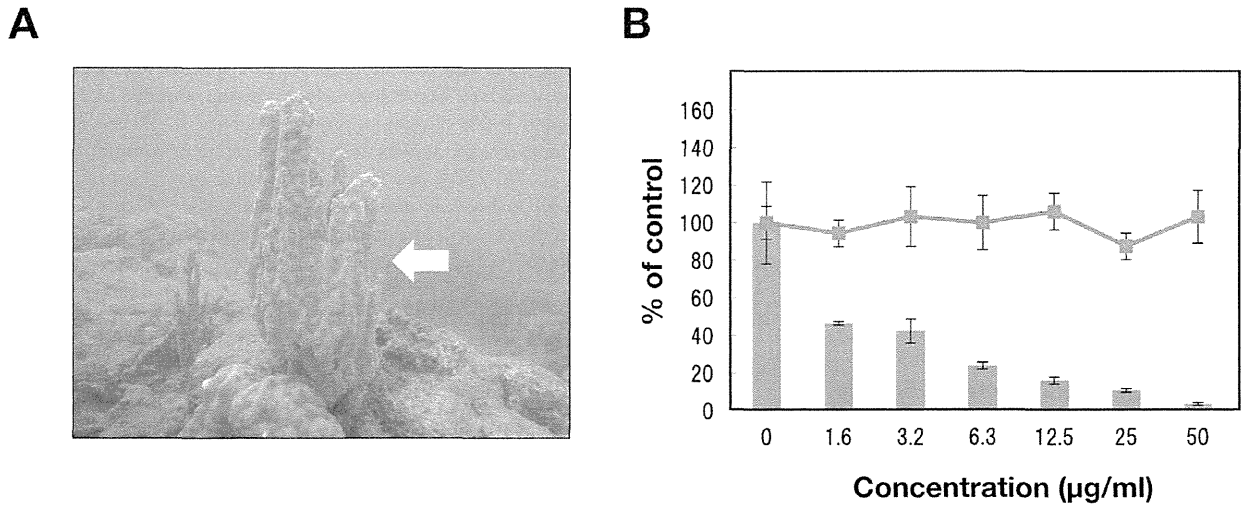

Figure 1. Effect of the extract prepared from a marine sponge on viral replication in the replicon cell line derived from viral genotype 1b. (A) *Amphimedon* sp. belongs to a marine sponge. The ethyl acetate fraction prepared from the marine organism was designated C-29EA in this study. (B) The Huh7 cell line, including the subgenomic replicon RNA of genotype 1b strain Con1, was incubated in medium containing various concentrations of C-29EA or DMSO (0). Luciferase and cytotoxicity assays were carried out as described in Materials and Methods. Error bars indicate standard deviation. The data represent three independent experiments.
doi:10.1371/journal.pone.0048685.g001

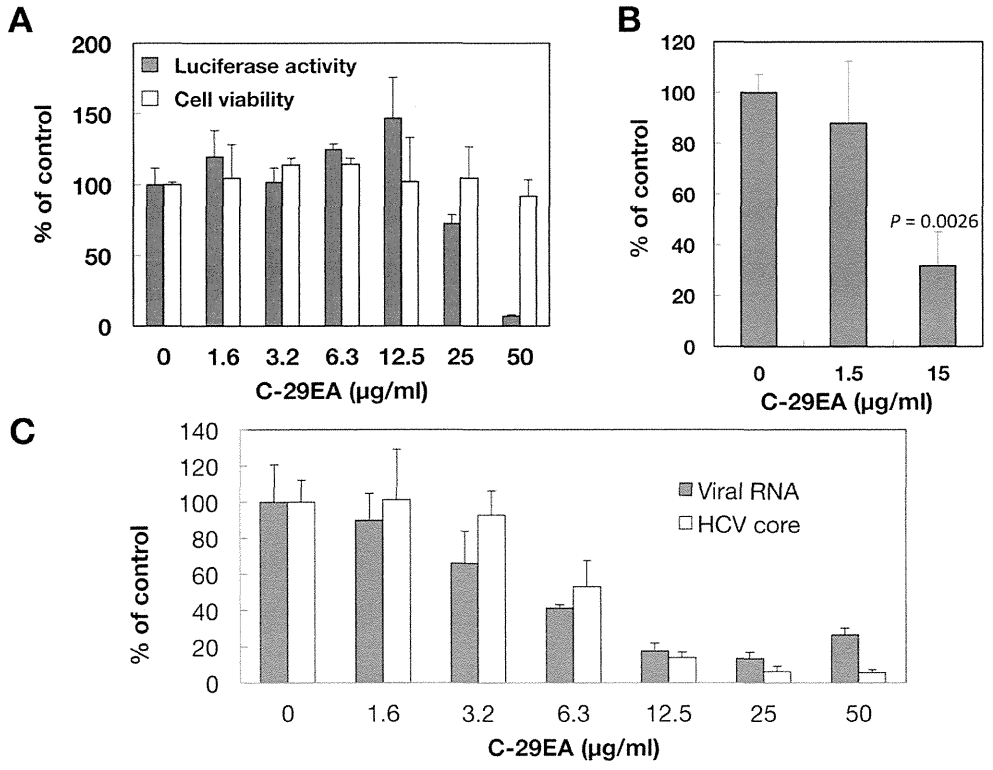

Figure 2. Effect of C-29EA extract on viral replication in the replicon cell line derived from viral genotype 2a. (A) The Huh7 cell line, including the subgenomic replicon RNA of genotype 2a strain JFH1, was incubated in medium containing various concentrations of C-29EA or DMSO (0). Luciferase and cytotoxicity assays were carried out as described in Materials and Methods. (B) The Huh7 OK1 cell line infected with HCVcc JFH1 was incubated with various concentrations of C-29EA or DMSO (0). The virus titers were determined by a focus-forming assay. The significance of differences in the means was determined by Student's *t*-test. (C) Amounts of viral RNA and core protein were estimated by qRT-PCR and ELISA, respectively. Error bars indicate standard deviation. The data represent three independent experiments. Treatment with DMSO corresponds to '0'.
doi:10.1371/journal.pone.0048685.g002

Table 2. Effect of C29EA on HCV replication.

HCV strain (genotype)	EC_{50} (μg/ml)[a]	CC_{50} (μg/ml)[b]	SI[c]
Con 1 (1b)	1.5	>50	>33.3
JFH1 (2a)	24.9	>50	>2.3

[a]: Fifty percent effective concentration based on the inhibition of HCV replication.
[b]: Fifty percent cytotoxicity concentration based on the reduction of cell viability.
[c]: SI, selectivity index (CC_{50}/EC_{50}).
doi:10.1371/journal.pone.0048685.t002

Effect of C-29EA on NS3 Protease Activity

Serine protease and helicase domains are respectively located on the N-terminal and C-terminal portions of NS3 [32]. Thus, we examined the effect of C-29EA on NS3 protease activity by using an NS3 protease assay based on FRET. NS3/4A serine protease was mixed with various concentrations of C-29EA. The initial velocity at each concentration of C-29EA was calculated during a 120 min reaction. The initial velocity in the absence of C-29EA represented 100% of relative protease activity. C-29EA decreased the serine protease activity in a dose-dependent manner (Fig. 7). The IC_{50} of C-29EA was 10.9 μg/ml, which is similar to the value estimated by helicase assay. These results suggest that C-29EA includes the compound(s) inhibiting the protease activity of NS3 in addition to the helicase activity.

Combination Antiviral Activity of C-29EA and Interferon-alpha

Treatment with C-29EA may potentiate inhibitory action of interferon-alpha, since it inhibited the protease and helicase activities of NS3 but not induce the interferon response as described above. Then, we examined effect of treatment using both interferon and C-29EA on HCV replication. The replication

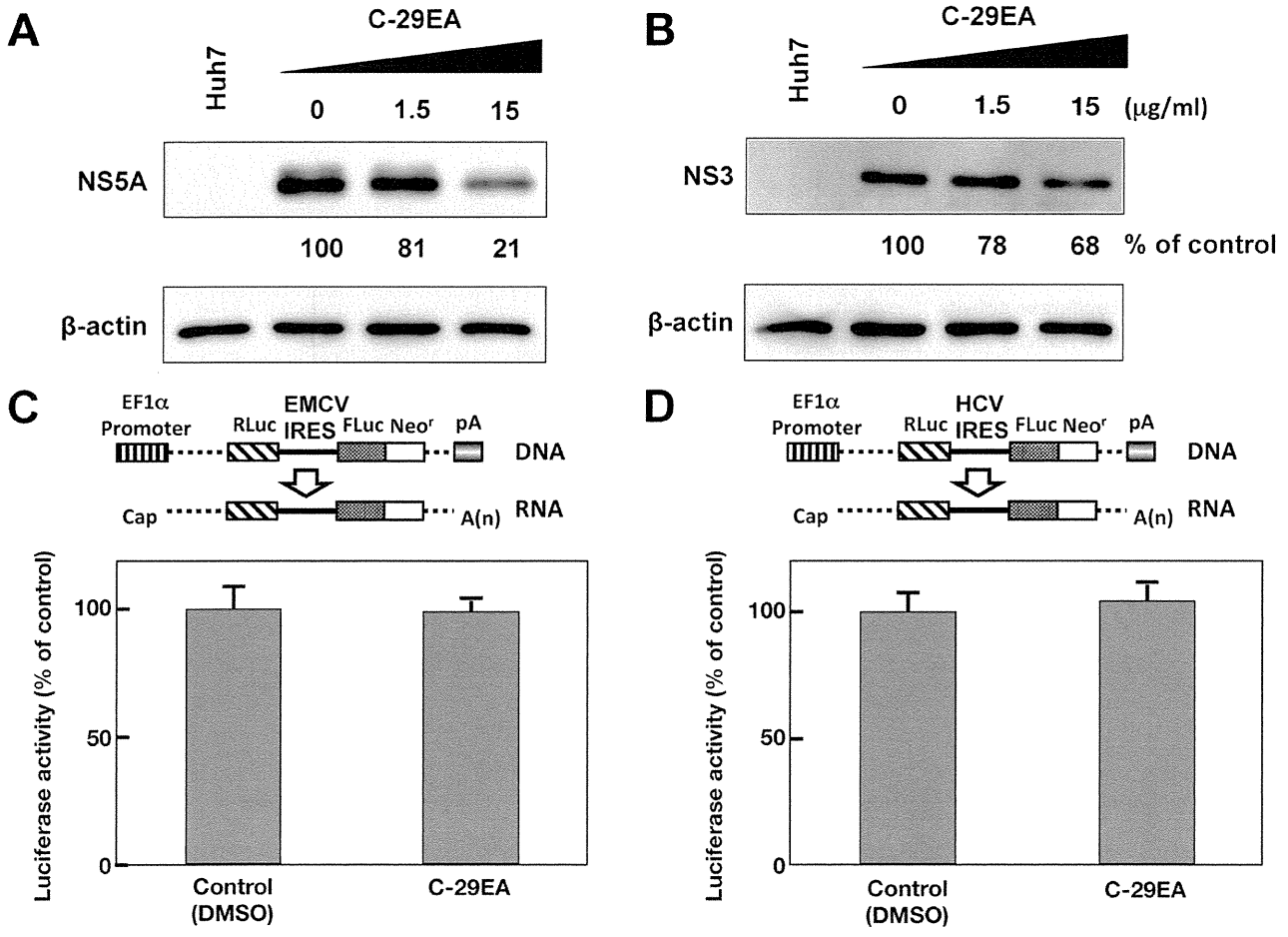

Figure 3. Effect of C-29EA on expression of viral proteins in replicon cell lines. The Huh7 replicon cell lines derived from genotype 1b (A) and 2a (B) were incubated with C-29EA at 37°C for 72 h. The treated cells were harvested and then subjected to Western blotting. Treatment with DMSO corresponds to '0'. The bicistronic gene is transcribed under the control of the elongation factor 1α (EF1α) promoter. The upstream cistron encoding *Renilla* luciferase (RLuc) is translated by a cap-dependent mechanism. The downstream cistron encodes the fusion protein (Feo), which consists of the firefly luciferase (Fluc) and neomycin phosphotransferase (Neo^r), and is translated under the control of the EMCV IRES (C) or HCV IRES (D). The Huh7 cell line transfected with the plasmid (each above the panel in C and D) was established in the presence of G418. The cells were incubated for 72 h without (control) and with 15 μg/ml of C-29EA. Firefly or *Renilla* luciferase activity was measured by the method described in Materials and Methods and was normalized by the protein concentration. F/R: relative ratio of firefly luciferase activity to *Renilla* luciferase activity. F/R is presented as a percentage of the control condition. Error bars indicate standard deviation. The data represent three independent experiments.
doi:10.1371/journal.pone.0048685.g003

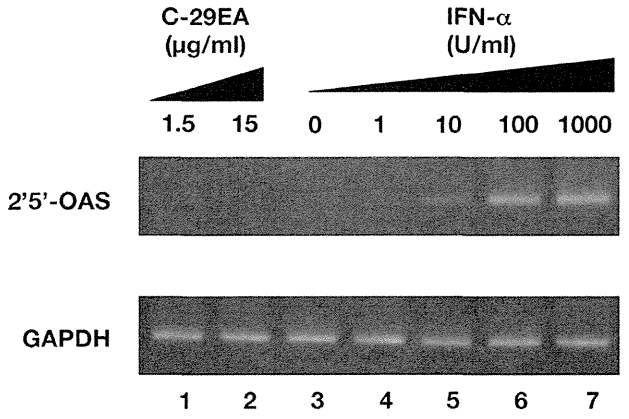

Figure 4. Effect of C-29EA on interferon signaling pathway. The Huh7 replicon cell line of genotype 1b was treated without (lane 3) or with 1, 10, 100, or 1000 U/mL interferon-alpha 2b (lanes 4–7), and 1.5 or 15 μg/ml C-29EA (lanes 1–2) for 48 h. Treatment with DMSO corresponds to '0'. The mRNAs of 2', 5'-OAS, and GAPDH as an internal control were detected by RT-PCR. Error bars indicate standard deviation. The data represent three independent experiments.
doi:10.1371/journal.pone.0048685.g004

of replicon was decreased in the presence of C-29EA or interferon-alpha and further decreased by combination treatment using interferon-alpha and C-29EA (Fig. 8A). Furthermore, we employed the isobologram method [33] to determine whether antiviral effect of the combination treatment exhibits additive or synergistic. EC_{90} values of interferon-alpha and C-29EA were estimated at 10.7 U/ml and 26.4 μg/ml, respectively, in the absence of each other. EC_{90} values of C-29EA in the presence of 0, 2.5 and 5 U/ml interferon-alpha were plotted to generate an isobole. Figure 8B shows that the isobole exhibits concave curvilinear, representing synergy but not additivity. These results suggest that combination treatment of interferon-alpha and C-29EA exhibits synergistic inhibition of HCV replication.

Discussion

Several natural products have been reported as anti-viral agents against HCV replication. Silbinin, epigallocatechin 3-gallate, and proanthocyanidins, which were prepared from milk thistle, green tea, and blueberry leaves, respectively, have exhibited inhibitory activity against HCV replication in cultured cells [34–37]. In our previous report, we identified manoalide as an anti-HCV agent from a marine sponge extract by high-throughput screening targeting NS3 helicase activity [38]. Manoalide inhibited ATPase, RNA binding, and NS3 helicase activity in enzymological assays. The EtOAc extract of the marine feather star also suppressed HCV replication in HCV replicon cell lines derived from genotype 1b, and it inhibited the RNA-binding activity but not the ATPase activity of NS3 helicase [30]. In this study, we screened 84 extracts of marine organisms for their ability to inhibit HCV replication in replicon cell lines and HCV cell culture system. Among these extracts, C-29EA, which was extracted from *Amphimedon* sp., most strongly inhibited HCV replication regardless of cytotoxicity. We previously reported that the EtOAc extract (SG1-23-1) of the feather star *Alloeocomatella polycladia* inhibited HCV replication with an EC_{50} of 22.9 to 44.2 μg/ml in HCV replicon cells derived from genotype 1b [30]. Treatment with C-29EA potently inhibited HCV replication with an EC_{50} of 1.5 μg/ml and with an SI of more than 33.3 in the replicon cell line derived from genotype 1b, regardless of cytotoxicity (Fig. 1B and Table 2). However, C-29EA exhibited an EC_{50} of 24.9 μg/ml in a replicon cell line derived from genotype 2a at a weaker level than in the replicon cell line derived from genotype 1b (Figs. 1 and 2), suggesting that the ability of C-29EA to suppress HCV replication is dependent on the viral genotype or strain.

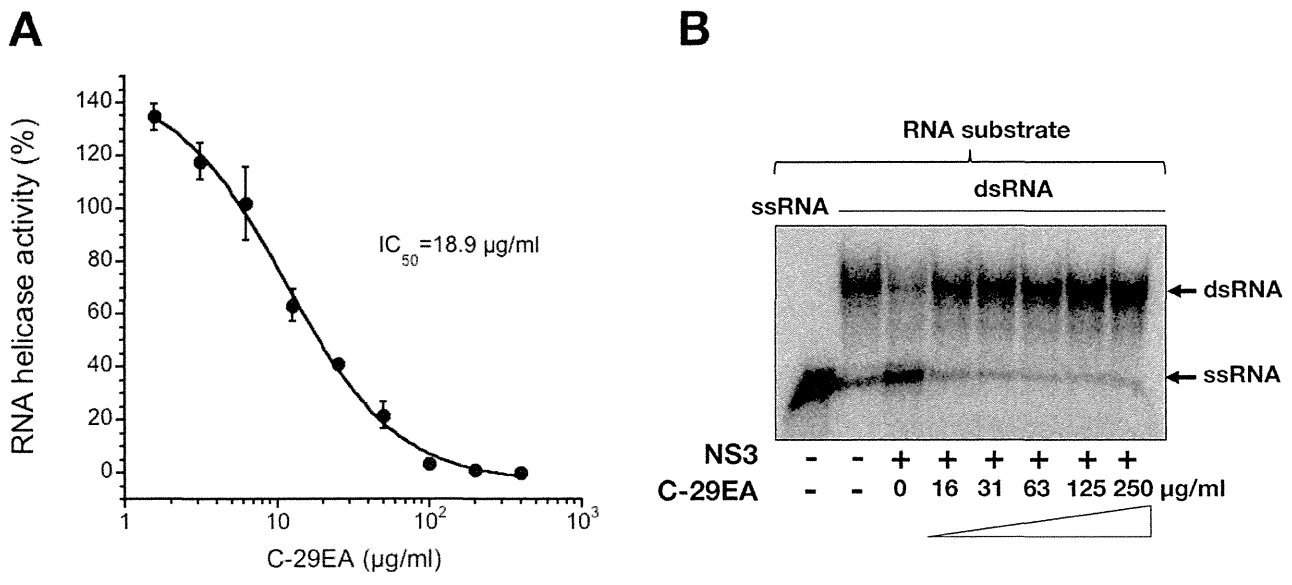

Figure 5. Effect of C-29EA on unwinding activity of NS3 helicase. (A) NS3 helicase activity was measured by PET assay. The reactions were carried out in the absence or presence of C-29EA. Helicase activity in the absence of C-29EA was defined as 100% helicase activity. Treatment with DMSO corresponds to '0'. The data are presented as the mean ± standard deviation for three replicates. (B) The unwinding activity of NS3 helicase was measured by an RNA unwinding assay using radioisotope-labeled RNA. The heat-denatured single-strand RNA (26-mer) and the partial duplex RNA substrate were applied to lanes 1 and 2, respectively. The duplex RNA was reacted with NS3 (300 nM) in the presence of C-29EA (lanes 4–9, 16–250 μg/ml). The resulting samples were subjected to native polyacrylamide gel electrophoresis. Treatment with DMSO corresponds to '0'.
doi:10.1371/journal.pone.0048685.g005

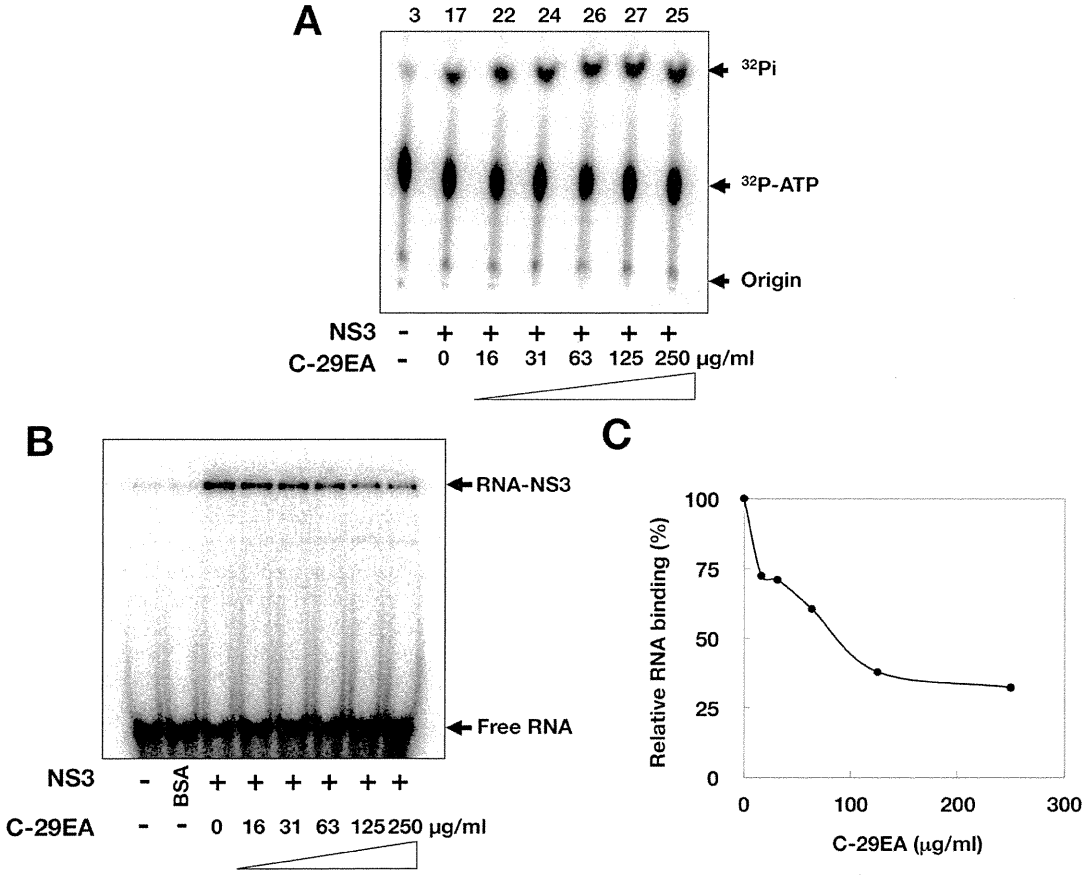

Figure 6. Effect of C-29EA on ATPase and RNA-binding activities of NS3 helicase. (A) The reaction mixtures were incubated with [γ-^{32}P] ATP as described in Materials and Methods. The reaction mixtures were subjected to thin-layer chromatography. The start positions and migrated positions of ATP and free phosphoric acid are indicated as 'Origin', '^{32}P-ATP', and '^{32}P-Pi', respectively, on the right side of the figure. The data represent three independent experiments. Treatment with DMSO corresponds to '0'. (B) Gel mobility shift assay for RNA-binding activity of NS3 helicase. The reaction was carried out with 0.5 nM labeled ssRNA at the indicated concentrations of C-29EA or DMSO. The reaction mixture was subjected to gel mobility shift assay. (C) The relative RNA-binding ability was calculated with band densities in each lane and presented as a percentage of RNA-NS3 in the total density. The data represent three independent experiments. Treatment with DMSO corresponds to '0'.
doi:10.1371/journal.pone.0048685.g006

HCV NS3 is well known to play a crucial role in viral replication through helicase and protease activities [5,39]. The N-terminal third of NS3 is responsible for serine protease activity in order to process the C-terminal portion of polyprotein containing viral nonstructural proteins [32]. The remaining portion of NS3 exhibits ATPase and RNA-binding activities responsible for helicase activity, which is involved in unwinding double-stranded RNA during replication of genomic viral RNA [40–42]. A negative-strand RNA is synthesized based on a viral genome (positive strand) after viral particles in the infected cells are uncoated, and is then used itself as a template to synthesize a positive-stranded RNA, which is translated or packaged into viral particles. Thus, both helicase and protease activities of NS3 are critical for HCV replication and could be targeted for the development of antiviral agents against HCV.

NS3 helicase activity was inhibited by treatment with C-29EA in a dose-dependent manner with an IC_{50} of 18.9 μg/ml (Fig. 5A). RNA-binding activity, but not ATPase activity, was inhibited by treatment with C-29EA (Fig. 6). Treatment with C-29EA did not significantly affect the HCV-IRES activity and did not induce interferon-stimulated gene 2′,5′-OAS (Figs. 3 and 4). Furthermore, the serine protease activity of NS3 was inhibited by using C-29EA with an IC_{50} of 10.9 μg/ml (Fig. 7). These results suggest that *Amphimedon* sp. includes the unknown compound(s) that could suppress NS3 enzymatic activity to inhibit HCV replication. Although the mechanism by which treatment with C-29EA could inhibit HCV replication has not yet been revealed, the unknown compound(s) may be associated with the inhibition of NS3 protease and helicase, leading to the suppression of HCV replication. However, other effects of extract C-29EA on HCV replication could not be excluded in this study.

The compound 1-N, 4-N-bis [4-(1H-benzimidazol-2-yl)phenyl] benzene-1,4-dicarboxamide, which is designated as $(BIP)_2B$, was reported to be a potent and selective inhibitor of HCV NS3 helicase [43]. This compound competitively decreases the binding ability of HCV NS3 helicase to nucleic acids. The compound $(BIP)_2B$ inhibited RNA-induced stimulation of ATPase, although it did not directly affect the ATP hydrolysis activity of NS3 helicase. Thus, $(BIP)_2B$ could not affect ATPase activity without RNA or with a high concentration of RNA. Treatment with C-29EA inhibited helicase activity and viral replication but not ATPase activity (Figs. 1B, 2, 5, and 6). This extract suppressed the binding of RNA to helicase but exhibited no suppression of ATPase by NS3 helicase. Thus, the inhibitory action of extract C-29EA seems

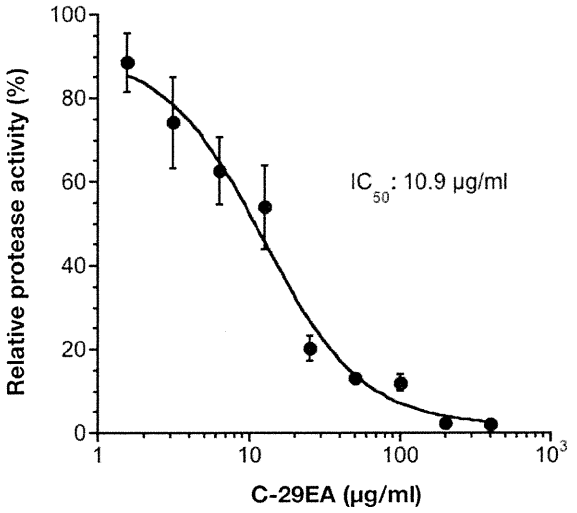

Figure 7. Effect of C-29EA on the activity of NS3 serine protease. NS3/4A serine protease was mixed with various concentrations of C-29EA or DMSO (0) in the reaction mixture and then incubated at 37°C for 120 min. The initial velocity at each concentration of C-29EA was calculated during 120 min reaction. The initial velocity in the absence of C-29EA was defined as 100% of relative protease activity. The data are presented as the mean ± standard deviation for three replicates.
doi:10.1371/journal.pone.0048685.g007

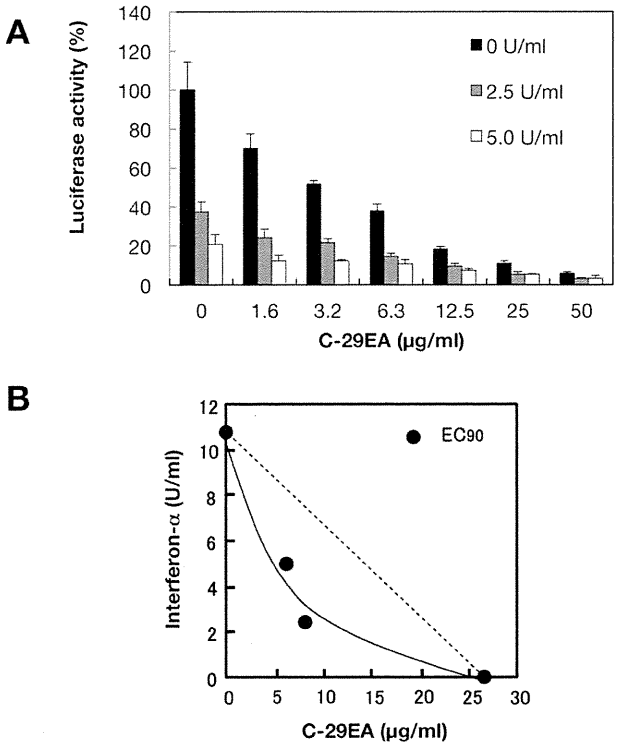

Figure 8. Effect of C-29EA on the antiviral activity of interferon-alpha. (A) The Huh7 cell line, including the subgenomic replicon RNA of genotype 1b strain Con1, was incubated in medium containing various concentrations of C-29EA or DMSO (0) in the presence or the absence of interferon-alpha. Luciferase assay were carried out as described in Materials and Methods. Error bars indicate standard deviation. The data represent three independent experiments. (B) Isobole plots of 90% inhibition of HCV replication. The broken line indicates the additive effect in the isobologram.
doi:10.1371/journal.pone.0048685.g008

different from that of $(BIP)_2B$. The quinolone derivative QU663 was reported to inhibit the unwinding activity of NS3 helicase by binding to an RNA-binding groove irrespective of its own ATPase activity [44]. The compound QU663 may competitively bind the RNA-binding site of NS3 but not affect ATPase activity, resulting in the inhibition of unwinding activity. In this study, treatment with C-29EA inhibited the RNA-binding activities of NS3 helicase but did not affect ATPase activity (Fig. 6). Furthermore, treatment with C-29EA suppressed the viral replication of HCV in an HCV cell culture system derived from several virus strains (Figs. 1 and 2, Table 2). The mechanism of C-29EA on the inhibition of NS3 helicase may be similar to that of compound QU663.

It is unknown whether one or several molecules included in C-29EA are critical for the inhibition of protease and helicase activities. The serine protease NS3/4A is one of the viral factors targeted for development into antiviral agents. Improvements in HCV therapy over the past several years have resulted in FDA approval of telaprevir (VX-950) [15,45] and boceprevir (SCH503034) [46,47]. Several studies suggest that the activities of NS3/4A protease and helicase in the full-length molecule enhance each other [48,49]. The NS3/4A protease has formed a complex with macrocyclic acylsulfonamide inhibitors [50,51]. Schiering et al. recently reported the structure of full-length NS3/4A in complex with a macrocyclic acylsulfonamide protease inhibitor [52], although the structure of full-length HCV NS3/4A in complex with a protease inhibitor has not been reported. The inhibitor binds to the active site of the protease, while the P4-capping and P2 moieties of the inhibitor are exposed toward the helicase interface and interact with both protease and helicase residues [52]. An unknown compound included in C-29EA might interact with both protease and helicase domains of NS3 to inhibit their activities. However, our data in this study have not excluded the possibility that several compounds included in C-29EA are related to the inhibition of protease and helicase of NS3/4A.

In conclusion, we showed that the EtOAc extract from *Amphimedon* sp. significantly inhibits HCV replication by suppressing viral helicase and protease activities. The purification of an inhibitory compound from the extract of *Amphimedon* sp. will be necessary in order to improve its efficacy by chemical modification.

Materials and Methods

Preparation of Extracts from Marine Organisms

All marine organisms used in this study were hand-collected by scuba diving off islands in Okinawa Prefecture, Japan. No specific permits were required for the described field studies. We do not have to obtain a local government permit to collect invertebrates except for stony corals and marine organisms for fisheries, which we did not collect in this study. The areas where we collected are not privately-owned or protected in any way. We did not collect any invertebrates listed in the red data book issued by Ministry of Environment, Japan. The sponges, tunicates, and soft corals used in this study are not listed at all. Hence, no specific permits are required for this collection in the same way as the previous report of Aratake et al. [53].

The sponge from which C-29EA was extracted was identified as *Amphimedon* sp. and deposited at Naturalis under the code RMNH POR 6100. Each specimen was soaked in acetone. The acetone-extract fraction prepared from each specimen was concentrated.

The resulting material was fractionated as an EtOAc- and water-soluble fraction. The water-soluble fraction was dried up and solubilized in MeOH. The EtOAc- and the MeOH-soluble fractions were used for screening. All samples were dried and then solubilized in dimethyl sulfoxide (DMSO) before testing.

Cell Lines and Virus

The following Huh-7-derived cell lines used in this study were maintained in Dulbecco's modified Eagle's medium containing 10% fetal calf serum and 0.5 mg/ml G418. The Lunet/Con1 LUN Sb #26 cell line, which harbors the subgenomic replicon RNA of the Con1 strain (genotype 1b), was kindly provided by Ralf Bartenschlager [26]. Huh7/ORN3-5B #24 cell line, which harbors the subgenomic replicon RNA of the O strain (genotype 1b) was reported previously [54] and used for screening in this study (Table 1). HCV replicon cell line derived from genotype 2a strain JFH1 was described previously [55]. The surviving cells were infected with the JFH-1 virus at a multiplicity of infection (moi) of 0.05. The viral RNA derived from the plasmid pJFH1 was transcribed and introduced into Huh7OK1 cells according to the method of Wakita et al. [56]. The infectivity of the JFH1 strain was determined by a focus-forming assay [56].

Quantitative Reverse-transcription PCR (qRT-PCR) and Estimation of Core Protein

The estimation of viral RNA genome was carried out by the method described previously [57] with slight modification. Total RNAs were prepared from cells and culture supernatants by using an RNeasy mini kit (QIAGEN, Tokyo, Japan) and QIAamp Viral RNA mini kit (QIAGEN), respectively. First-strand cDNA was synthesized by using a high capacity cDNA reverse transcription kit (Applied Biosystems, Carlsbad, CA, USA) with random primers. Each cDNA was estimated by using Platinum SYBR Green qPCR SuperMix UDG (Invitrogen, Carlsbad, CA, USA) according to the manufacturer's protocol. Fluorescent signals of SYBR Green were analyzed by using an ABI PRISM 7000 (Applied Biosystems). The HCV internal ribosomal entry site (IRES) region was amplified using the primer pair 5′-GAGTGTCGTGCAGCCTCCA -3′ and 5′- CACTCGCAAG-CACCCTATCA -3′. Expression of HCV core protein was determined by an enzyme-linked immunosorbent assay (ELISA) as described previously [57].

Determination of Luciferase Activity and Cytotoxicity in HCV Replicon Cells

HCV replicon cells were seeded at 2×10^4 cells per well in a 48-well plate 24 h before treatment. C-29EA was added to the culture medium at various concentrations. The treated cells were harvested 72 h post-treatment and lysed in cell culture lysis reagent (Promega, Madison, WI, USA) or *Renilla* luciferase assay lysis buffer (Promega). Luciferase activity in the harvested cells was estimated with a luciferase assay system (Promega) or a *Renilla* luciferase assay system (Promega). The resulting luminescence was detected by the Luminescencer-JNR AB-2100 (ATTO, Tokyo, Japan) and corresponded to the expression level of the HCV replicon. Cell viability was measured by a dimethylthiazol carboxymethoxy-phenylsulfophenyl tetrazolium (MTS) assay using a CellTiter 96 aqueous one-solution cell proliferation assay kit (Promega).

Effects on Activities of Internal Ribosome Entry Site (IRES)

Huh7 cells were transfected with pEF.Rluc.HCV.IRES.Feo or pEF.Rluc.EMCV.IRES.Feo and then were established in medium containing 0.25 mg/ml G418, as described previously [58]. These cell lines were seeded at 2×10^4 cells per well in a 48-well plate 24 h before treatment, treated with 15 μg/ml extract C-29EA, and then harvested at 72 h post-treatment. The firefly luciferase activities were measured with a luciferase assay system (Promega). The total protein concentration was measured using the BCA Protein Assay Reagent Kit (Thermo Scientific, Rockford, IL, USA) to normalize luciferase activity.

Western Blotting and Reverse-transcription Polymerase Chain Reaction (RT-PCR)

Western blotting was carried out by a method described previously [30]. The antibodies to NS3 (clone 8G-2, mouse monoclonal, Abcam, Cambridge, UK), NS5A (clone 256-A, mouse monoclonal, ViroGen, Watertown, MA, USA), and beta-actin were purchased from Cell Signaling Technology (rabbit polyclonal, Danvers, MA, USA) and were used as the primary antibodies in this study. RT-PCR was carried out by a method described previously [30,58].

Assays for RNA Helicase, ATPase, and RNA-binding Activities

A continuous fluorescence assay based on photoinduced electron transfer (PET) was described previously [29] and was slightly modified with regard to the reaction mixture [30]. The NS3 RNA unwinding assay was carried out by the method of Gallinari et al. [59] with slight modifications [30]. NS3 ATPase activity was determined by the method of Gallinari et al. [59] with slight modifications [30]. RNA binding to NS3 helicase was analyzed by a gel mobility shift assay [30,31]. The gene encoding NS3 helicase was amplified from the viral genome of genotype 1b and was introduced into a plasmid for the expression of a recombinant protein [38,60]. The radioactive band was visualized with the Image Reader FLA-9000 and quantified by Multi Gauge V 3.11 software.

NS3 Protease Assay

The fluorescence NS3 serine protease assay based on fluorescence resonance energy transfer (FRET) was carried out by the modified method using the SensoLyte™ 520 HCV protease assay kit (AnaSpec, Fremont, CA, USA). In brief, NS3 protein with a two-fold excess of NS4A cofactor peptide (Pep4AK) was prepared in 1× assay buffer provided with the kit. HCV NS3/4A protease was mixed with increasing concentrations of C-29EA and incubated at 37°C for 15 min. The reaction was started by adding the 5-FAM/QXL 520 substrate to the reaction mixture containing 180 nM HCV NS3/4A protease and various concentrations (0–400 μg/ml) of C-29EA. The resulting mixture (20 μl) was incubated at 37°C for 120 min using a LightCycler 1.5 (Roche Diagnostics, Basel, Switzerland). The fluorescence intensity was recorded every minute for 120 min. The NS3 serine protease activity was calculated as the initial reaction velocity and presented as a percentage of relative activity to that of the control examined with DMSO solvent but not C-29EA, in the same way as described in the fluorescence helicase assay [29].

Analysis of Drug-drug Interaction

The effects of drug combinations were evaluated using the isobologram method [33]. Various doses of C-29EA and interferon-alpha on 90% inhibition of HCV replication were combined to generate an isoeffect curve (isobole) to determine drug–drug interaction. Concave, linear, and convex curves exhibit synergy, additivity, and antagonism, respectively.

Statistical Analysis

The results are expressed as the mean ± standard deviation. The significance of differences in the means was determined by Student's *t*-test.

Acknowledgments

We thank T. Wakita and R. Bartenschlager for kindly providing the virus, cell lines, and plasmids; and H. Kasai and I. Katoh for their helpful comments and discussions.

Author Contributions

Conceived and designed the experiments: MN MT YS ST NA NN AY JT KM. Performed the experiments: YF KAS AF YM OF HT AY. Analyzed the data: MI NK NS SM NE. Wrote the paper: YF AY JT KM. Collected marine organisms: JT. Identified the sponge: NJdV.

References

1. Baldo V, Baldovin T, Trivello R, Floreani A (2008) Epidemiology of HCV infection. Curr Pharm Des 14: 1646–1654.
2. Seeff LB (2002) Natural history of chronic hepatitis C. Hepatology 36: S35–46.
3. Moriishi K, Matsuura Y (2012) Exploitation of lipid components by viral and host proteins for hepatitis C virus infection. Front Microbiol 3: 54.
4. Tsukiyama-Kohara K, Iizuka N, Kohara M, Nomoto A (1992) Internal ribosome entry site within hepatitis C virus RNA. J Virol 66: 1476–1483.
5. Kim DW, Gwack Y, Han JH, Choe J (1995) C-terminal domain of the hepatitis C virus NS3 protein contains an RNA helicase activity. Biochem Biophys Res Commun 215: 160–166.
6. Kanai A, Tanabe K, Kohara M (1995) Poly(U) binding activity of hepatitis C virus NS3 protein, a putative RNA helicase. FEBS Lett 376: 221–224.
7. Manns MP, Wedemeyer H, Cornberg M (2006) Treating viral hepatitis C: efficacy, side effects, and complications. Gut 55: 1350–1359.
8. McHutchison JG, Everson GT, Gordon SC, Jacobson IM, Sulkowski M, et al. (2009) Telaprevir with peginterferon and ribavirin for chronic HCV genotype 1 infection. N Engl J Med 360: 1827–1838.
9. Zeuzem S, Hultcrantz R, Bourliere M, Goeser T, Marcellin P, et al. (2004) Peginterferon alfa-2b plus ribavirin for treatment of chronic hepatitis C in previously untreated patients infected with HCV genotypes 2 or 3. J Hepatol 40: 993–999.
10. Asselah T, Marcellin P (2011) New direct-acting antivirals' combination for the treatment of chronic hepatitis C. Liver Int 31 Suppl 1: 68–77.
11. Jazwinski AB, Muir AJ (2011) Direct-acting antiviral medications for chronic hepatitis C virus infection. Gastroenterol Hepatol (N Y) 7: 154–162.
12. Lange CM, Sarrazin C, Zeuzem S (2010) Review article: specifically targeted anti-viral therapy for hepatitis C - a new era in therapy. Aliment Pharmacol Ther 32: 14–28.
13. Hofmann WP, Zeuzem S (2011) A new standard of care for the treatment of chronic HCV infection. Nat Rev Gastroenterol Hepatol 8: 257–264.
14. Kwong AD, Kauffman RS, Hurter P, Mueller P (2011) Discovery and development of telaprevir: an NS3–4A protease inhibitor for treating genotype 1 chronic hepatitis C virus. Nat Biotechnol 29: 993–1003.
15. Jacobson IM, McHutchison JG, Dusheiko G, Di Bisceglie AM, Reddy KR, et al. (2011) Telaprevir for previously untreated chronic hepatitis C virus infection. N Engl J Med 364: 2405–2416.
16. Sarrazin C, Hezode C, Zeuzem S, Pawlotsky JM (2012) Antiviral strategies in hepatitis C virus infection. J Hepatol 56 Suppl 1: S88–100.
17. Chen ST, Wu PA (2012) Severe Cutaneous Eruptions on Telaprevir. J Hepatol 57: 470–472.
18. Kieffer TL, Kwong AD, Picchio GR (2010) Viral resistance to specifically targeted antiviral therapies for hepatitis C (STAT-Cs). J Antimicrob Chemother 65: 202–212.
19. Thompson AJ, McHutchison JG (2009) Antiviral resistance and specifically targeted therapy for HCV (STAT-C). J Viral Hepat 16: 377–387.
20. Chin YW, Balunas MJ, Chai HB, Kinghorn AD (2006) Drug discovery from natural sources. AAPS J 8: E239–253.
21. Koehn FE, Carter GT (2005) The evolving role of natural products in drug discovery. Nat Rev Drug Discov 4: 206–220.
22. Li JW, Vederas JC (2009) Drug discovery and natural products: end of an era or an endless frontier? Science 325: 161–165.
23. Donia M, Hamann MT (2003) Marine natural products and their potential applications as anti-infective agents. Lancet Infect Dis 3: 338–348.
24. Molinski TF, Dalisay DS, Lievens SL, Saludes JP (2009) Drug development from marine natural products. Nat Rev Drug Discov 8: 69–85.
25. Mayer AM, Glaser KB, Cuevas C, Jacobs RS, Kem W, et al. (2010) The odyssey of marine pharmaceuticals: a current pipeline perspective. Trends Pharmacol Sci 31: 255–265.
26. Frese M, Barth K, Kaul A, Lohmann V, Schwarzle V, et al. (2003) Hepatitis C virus RNA replication is resistant to tumour necrosis factor-alpha. J Gen Virol 84: 1253–1259.
27. Blight KJ, Kolykhalov AA, Rice CM (2000) Efficient initiation of HCV RNA replication in cell culture. Science 290: 1972–1974.
28. Guo JT, Bichko VV, Seeger C (2001) Effect of alpha interferon on the hepatitis C virus replicon. J Virol 75: 8516–8523.
29. Tani H, Akimitsu N, Fujita O, Matsuda Y, Miyata R, et al. (2009) High-throughput screening assay of hepatitis C virus helicase inhibitors using fluorescence-quenching phenomenon. Biochem Biophys Res Commun 379: 1054–1059.
30. Yamashita A, Salam KA, Furuta A, Matsuda Y, Fujita O, et al. (2012) Inhibition of hepatitis C virus replication and NS3 helicase by the extract of the feather star *Alloeocomatella polycladia*. Mar Drugs 10: 744–761.
31. Huang Y, Liu ZR (2002) The ATPase, RNA unwinding, and RNA binding activities of recombinant p68 RNA helicase. J Biol Chem 277: 12810–12815.
32. Failla C, Tomei L, De Francesco R (1994) Both NS3 and NS4A are required for proteolytic processing of hepatitis C virus nonstructural proteins. J Virol 68: 3753–3760.
33. Leu GZ, Lin TY, Hsu JT (2004) Anti-HCV activities of selective polyunsaturated fatty acids. Biochem Biophys Res Commun 318: 275–280.
34. Ahmed-Belkacem A, Ahnou N, Barbotte L, Wychowski C, Pallier C, et al. (2010) Silibinin and related compounds are direct inhibitors of hepatitis C virus RNA-dependent RNA polymerase. Gastroenterology 138: 1112–1122.
35. Ciesek S, von Hahn T, Colpitts CC, Schang LM, Friesland M, et al. (2011) The green tea polyphenol, epigallocatechin-3-gallate, inhibits hepatitis C virus entry. Hepatology 54: 1947–1955.
36. Takeshita M, Ishida Y, Akamatsu E, Ohmori Y, Sudoh M, et al. (2009) Proanthocyanidin from blueberry leaves suppresses expression of subgenomic hepatitis C virus RNA. J Biol Chem 284: 21165–21176.
37. Wagoner J, Negash A, Kane OJ, Martinez LE, Nahmias Y, et al. (2010) Multiple effects of silymarin on the hepatitis C virus lifecycle. Hepatology 51: 1912–1921.
38. Salam KA, Furuta A, Noda N, Tsuneda S, Sekiguchi Y, et al. (2012) Inhibition of Hepatitis C Virus NS3 Helicase by Manoalide. J Nat Prod 75: 650–654.
39. Bartenschlager R, Ahlborn-Laake L, Mous J, Jacobsen H (1993) Nonstructural protein 3 of the hepatitis C virus encodes a serine-type proteinase required for cleavage at the NS3/4 and NS4/5 junctions. J Virol 67: 3835–3844.
40. Belon CA, Frick DN (2009) Helicase inhibitors as specifically targeted antiviral therapy for hepatitis C. Future Virol 4: 277–293.
41. Frick DN (2007) The hepatitis C virus NS3 protein: a model RNA helicase and potential drug target. Curr Issues Mol Biol 9: 1–20.
42. Kwong AD, Rao BG, Jeang KT (2005) Viral and cellular RNA helicases as antiviral targets. Nat Rev Drug Discov 4: 845–853.
43. Belon CA, High YD, Lin TI, Pauwels F, Frick DN (2010) Mechanism and specificity of a symmetrical benzimidazolephenylcarboxamide helicase inhibitor. Biochemistry 49: 1822–1832.
44. Maga G, Gemma S, Fattorusso C, Locatelli GA, Butini S, et al. (2005) Specific targeting of hepatitis C virus NS3 RNA helicase. Discovery of the potent and selective competitive nucleotide-mimicking inhibitor QU663. Biochemistry 44: 9637–9644.
45. Reesink HW, Zeuzem S, Weegink CJ, Forestier N, van Vliet A, et al. (2006) Rapid decline of viral RNA in hepatitis C patients treated with VX-950: a phase Ib, placebo-controlled, randomized study. Gastroenterology 131: 997–1002.
46. Malcolm BA, Liu R, Lahser F, Agrawal S, Belanger B, et al. (2006) SCH 503034, a mechanism-based inhibitor of hepatitis C virus NS3 protease, suppresses polyprotein maturation and enhances the antiviral activity of alpha interferon in replicon cells. Antimicrob Agents Chemother 50: 1013–1020.
47. Njoroge FG, Chen KX, Shih NY, Piwinski JJ (2008) Challenges in modern drug discovery: a case study of boceprevir, an HCV protease inhibitor for the treatment of hepatitis C virus infection. Acc Chem Res 41: 50–59.
48. Beran RK, Pyle AM (2008) Hepatitis C viral NS3–4A protease activity is enhanced by the NS3 helicase. J Biol Chem 283: 29929–29937.
49. Beran RK, Serebrov V, Pyle AM (2007) The serine protease domain of hepatitis C viral NS3 activates RNA helicase activity by promoting the binding of RNA substrate. J Biol Chem 282: 34913–34920.
50. Cummings MD, Lindberg J, Lin TI, de Kock H, Lenz O, et al. (2010) Induced-fit binding of the macrocyclic noncovalent inhibitor TMC435 to its HCV NS3/NS4A protease target. Angew Chem Int Ed Engl 49: 1652–1655.
51. Romano KP, Ali A, Royer WE, Schiffer CA (2010) Drug resistance against HCV NS3/4A inhibitors is defined by the balance of substrate recognition versus inhibitor binding. Proc Natl Acad Sci U S A 107: 20986–20991.
52. Schiering N, D'Arcy A, Villard F, Simic O, Kamke M, et al. (2011) A macrocyclic HCV NS3/4A protease inhibitor interacts with protease and helicase residues in the complex with its full-length target. Proc Natl Acad Sci U S A 108: 21052–21056.

53. Aratake S, Tomura T, Saitoh S, Yokokura R, Kawanishi Y, et al. (2012) Soft coral Sarcophyton (Cnidaria: Anthozoa: Octocorallia) species diversity and chemotypes. PLoS One 7: e30410.
54. Ikeda M, Abe K, Dansako H, Nakamura T, Naka K, et al. (2005) Efficient replication of a full-length hepatitis C virus genome, strain O, in cell culture, and development of a luciferase reporter system. Biochem Biophys Res Commun 329: 1350–1359.
55. Nishimura-Sakurai Y, Sakamoto N, Mogushi K, Nagaie S, Nakagawa M, et al. (2010) Comparison of HCV-associated gene expression and cell signaling pathways in cells with or without HCV replicon and in replicon-cured cells. J Gastroenterol 45: 523–536.
56. Wakita T, Pietschmann T, Kato T, Date T, Miyamoto M, et al. (2005) Production of infectious hepatitis C virus in tissue culture from a cloned viral genome. Nat Med 11: 791–796.
57. Moriishi K, Shoji I, Mori Y, Suzuki R, Suzuki T, et al. (2010) Involvement of PA28gamma in the propagation of hepatitis C virus. Hepatology 52: 411–420.
58. Jin H, Yamashita A, Maekawa S, Yang P, He L, et al. (2008) Griseofulvin, an oral antifungal agent, suppresses hepatitis C virus replication in vitro. Hepatol Res 38: 909–918.
59. Gallinari P, Brennan D, Nardi C, Brunetti M, Tomei L, et al. (1998) Multiple enzymatic activities associated with recombinant NS3 protein of hepatitis C virus. J Virol 72: 6758–6769.
60. Nishikawa F, Funaji K, Fukuda K, Nishikawa S (2004) In vitro selection of RNA aptamers against the HCV NS3 helicase domain. Oligonucleotides 14: 114–129.

JOURNAL OF VIRAL HEPATITIS

Journal of Viral Hepatitis, 2012 doi:10.1111/j.1365-2893.2012.01649.x

IL-28B (IFN-λ3) and IFN-α synergistically inhibit HCV replication

H. Shindo,[1] S. Maekawa,[1] K. Komase,[1] M. Miura,[1] M. Kadokura,[1] R. Sueki,[1] N. Komatsu,[1] K. Shindo,[1] F. Amemiya,[1] Y. Nakayama,[1] T. Inoue,[1] M. Sakamoto,[1] A. Yamashita,[2] K. Moriishi[2] and N. Enomoto[1] [1]*First Department of Internal Medicine, University of Yamanashi, Yamanashi, Japan; and* [2]*Department of Microbiology, University of Yamanashi, Yamanashi, Japan*

Received March 2012; accepted for publication June 2012

SUMMARY. Genetic variation in the IL-28B (interleukin-28B; interferon lambda 3) region has been associated with sustained virological response (SVR) rates in patients with chronic hepatitis C treated with peginterferon-α and ribavirin. However, the mechanisms by which polymorphisms in the IL-28B gene region affect host antiviral responses are not well understood. Using the HCV 1b and 2a replicon system, we compared the effects of IFN-λs and IFN-α on HCV RNA replication. The anti-HCV effect of IFN-λ3 and IFN-α in combination was also assessed. Changes in gene expression induced by IFN-λ3 and IFN-α were compared using cDNA microarray analysis. IFN-λs at concentrations of 1 ng/mL or more exhibited concentration- and time-dependent HCV inhibition. In combination, IFN-λ3 and IFN-α had a synergistic anti-HCV effect; however, no synergistic enhancement was observed for interferon-stimulated response element (ISRE) activity or upregulation of interferon-stimulated genes (ISGs). With respect to the time course of ISG upregulation, the peak of IFN-λ3-induced gene expression occurred later and lasted longer than that induced by IFN-α. In addition, although the genes upregulated by IFN-α and IFN-λ3 were similar to microarray analysis, interferon-stimulated gene expression appeared early and was prolonged by combined administration of these two IFNs. In conclusion, IFN-α and IFN-λ3 in combination showed synergistic anti-HCV activity *in vitro*. Differences in time-dependent upregulation of these genes might contribute to the synergistic antiviral activity.

Keywords: HCV, IFN-λ, IL-28B, ISG, synergistic inhibition, microarray.

INTRODUCTION

In 2009, reports from three genome-wide association studies revealed that several single-nucleotide polymorphisms (SNPs) (rs12979860, rs12980275 and rs8099917) around the IL-28B (interleukin-28B; interferon lambda 3) gene are strongly associated with sustained viral response (SVR) to PEG-IFN and RBV treatment for chronic hepatitis C [1–3]. Specifically, patients with the TG or GG genotype at rs8099917 infected with genotype 1b are more resistant to PEG-IFN and RBV treatment than patients with the TT genotype. IL-28B haplotypes were also reported to be strongly associated with spontaneous HCV clearance [1, 4, 5].

IL-28B is a member of the type III IFN family [6], consisting of IFN-λ1 (IL-29), IFN-λ2 (IL-28A) and IFN-λ3 (IL-28B). IFN-λs bind to their cognate receptor, composed of IL28R1 and IL10R2, and then activate the receptor-associated Janus-activated kinases (Jak) 1 and tyrosine kinase (Tyk) 2, leading to the activation of downstream signal transducer and activator of transcription (STAT) proteins, STAT1 and STAT2. Similar to type I IFN signalling, the Jak-STAT signalling pathway activates the IFN-stimulated response element (ISRE) within the promoter region of interferon-stimulated genes (ISGs) [7].

Concerning the functional role of IL-28B in HCV infection, two of *in vivo* studies assessed the correlation of IL-28A/B mRNA levels in whole blood and peripheral blood mononuclear cells (PBMC) with IL-28B haplotypes at position rs8099917. IL-28A mRNA and IL-28B mRNA levels in subjects with the TT genotype were higher than in subjects with other genotypes (TG or GG), suggesting an association between higher amounts of endogenous IFN-λs and HCV clearance [2, 3]. On the other hand, subjects

Abbreviations: DMEM, Dulbecco's modified Eagle's medium; FBS, foetal bovine serum; ISG, interferon-stimulated genes; MTS, dimethylthiazol carboxymethoxyphenyl sulphophenyl tetrazolium; PBMC, peripheral blood mononuclear cells; SNP, single-nucleotide polymorphisms; STAT, signal transducer and activator of transcription; SVR, sustained viral response.

Correspondence: Shinya Maekawa, M.D., Ph.D., First Department of Internal Medicine, University of Yamanashi, 1110, Shimokato, Chuo, Yamanashi 409-3898, Japan. E-mail: maekawa@yamanashi.ac.jp

with the TT genotype at SNP rs8099917 were reported to have lower expression levels of ISGs in the liver during the pretreatment period as compared with subjects with the TG or GG genotypes [8]. Several *in vitro* studies support a direct role of IFN-λs in the control of HCV replication through the innate immune pathway. In a cell culture system, Marcello *et al.* [9] showed that IFN-λ1 inhibited HCV replication with similar kinetics to that of IFN-α, although IFN-λ1 induced stronger upregulation of ISGs and this effect lasted longer. Moreover, combinations of IFN-λ1 and IFN-α had a greater inhibitory effect on HCV replication compared with the individual agents [10].

As suggested by the studies performed to date, a change in IFN-λ3 expression might be a key mechanism by which IL-28B SNPs determine the response to PEG-IFN and RBV. Considering that IFN-λ1 plays a direct role in the control of HCV replication and that IFN-λ1 enhances the antiviral activity of IFN-α, it seems reasonable to speculate that IFN-λ3 plays a similar antiviral role. Therefore, in this study, we investigated the direct antiviral role of IFN-λ3 alone and in combination with IFN-α using an HCV replicon system. In addition, we used microarray analysis to investigate the influence of IFN-λ3, alone or in combination with IFN-α, on the regulation of ISG-mediated antiviral pathways.

MATERIALS AND METHODS

Cell culture and HCV replicon

The human hepatoma cell lines OR6 and Huh7.5.1 were maintained in Dulbecco's modified Eagle's medium (DMEM; Sigma, St. Louis, MO, USA) supplemented with 10% foetal bovine serum (FBS) at 37°C in 5% CO_2. JFH-1-infected Huh7.5.1 cells were grown in DMEM supplemented with 10% FBS. The OR6 cell line, harbouring full-length genotype 1b HCV RNA and co-expressing *Renilla* luciferase (ORN/C-5B/KE) [11], was established in the presence of 500 μg/mL G418 (Promega, Madison, WI, USA).

Reagents

IL-28A (IFN-λ2), IL-28B (IFN-λ3) and IL-29 (IFN-λ1) were obtained from R&D Systems (Minneapolis, MN, USA). IL-28A and IL-29 are recombinant proteins generated from an NSO-derived murine myeloma cell line, and IL-28B is a recombinant protein generated from the CHO cell line. Interferon alpha-2b (INTRON®A 300 IU) was obtained from Schering-Plough Corporation (Kenilworth, NJ, USA).

Reporter plasmids and luciferase assay

HCV replication in OR6 replicon cells was determined by monitoring *Renilla* luciferase activity (Promega). To monitor IFN signalling directed by the interferon-stimulated response element (ISRE), the plasmids pISRE-luc expressing firefly luciferase were cotransfected using FuGENE®6 Transfection Reagent (Roche, Indianapolis, IN, USA) following the manufacturer's protocol. Luciferase activity was quantified using the dual-luciferase assay system (Promega) and a GloMax 96 Microplate Luminometer (Promega). Assays were performed in triplicate, and the results were expressed as mean ± SD percentage of the control values.

Quantification of HCV core protein and RNA

We quantified HCV core protein in culture supernatant using Lumipulse Ortho HCV Ag (Ortho Clinical Diagnostics, Tokyo, Japan) as specified by the manufacturer. The principle of the measurement method is based on the chemiluminescent enzyme immunoassay (CLEIA) [12].

Real-time reverse transcription polymerase chain reaction (RT-PCR)

Intracellular genomic JFH-1 HCV RNA as well as cellular mRNA of IFI-6, IFIT1 (ISG56), DDX60, OAS2, Mx1 and USP18 was quantified by TaqMan RT-PCR. The cells were lysed and subjected to reverse transcription without purification of RNA using a Cells-to-Ct kit (Applied Biosystems, Foster City, CA, USA) according to the manufacturer's protocol. Quantitative PCR was performed in triplicate using a 7500 Real-Time PCR System (Applied Biosystems) and TaqMan Gene Expression Assays (Applied Biosystems) according to the manufacturer's instructions. The sequences of the sense and antisense primers and the TaqMan probe for 5′UTR region of HCV were 5′-TGCGG AACCGGTGAGTACA-3′, 5′-CTTAAGGTTTAGGATTCGTGCT CAT-3′ and 5′-(FAM)CACCCTATCAGGCAGTACCACAAGG CC(TAMRA)-3′, respectively. TaqMan probes for IFI-6, IFIT1 (ISG56), DDX60, OAS2, Mx1 and USP18 were purchased from Applied Biosystems. Primers for 18s rRNA (Applied Biosystems) were used as internal control.

Microarray analysis

OR6 replicon cells were harvested by centrifugation after exposure to 0.01 ng/mL IFN-α, 10 ng/mL IFN-λ3 or a combination of both for 6, 12, 24 and 48 h. Total RNA was isolated from cells using the RNeasy Mini Kit (Qiagen, Valencia, CA, USA). On-column DNase digestion was performed using the RNase-Free DNase Set (Qiagen). Quality control of extracted RNA was performed with the 2100 Bioanalyzer (Agilent Technologies, Palo Alto, CA, USA).

The RNA was then amplified and labelled using the Ambion® WT Expression Kit and GeneChip® WT Terminal Labelling and Control Kit (Affymetrix, Santa Clara, CA, USA). cDNA was synthesized, labelled and hybridized to the GeneChip® array according to the manufacturer's protocol, starting with 200-ng total RNA. The GeneChips were finally washed

and stained using the GeneChip® Fluidics Station 450 (Affymetrix) and then scanned with the GeneChip® Scanner 3000 7G (Affymetrix).

Affymetrix CEL files were imported into GeneSpring GX v.11.5 (Agilent Technologies, Santa Clara, CA, USA) analysis software. Data were normalized using robust multichip average analysis (RMA).

Dimethylthiazol carboxymethoxyphenyl sulphophenyl tetrazolium (MTS) assays

To evaluate the cell viability, dimethylthiazol carboxymethoxyphenyl sulphophenyl tetrazolium (MTS) assays were performed using a CellTiter 96 AQueous One Solution Cell Proliferation Assay kit (Promega) according to the manufacturer's instructions.

Statistical analyses

Statistical analyses were performed using an unpaired, two-tailed Student's *t*-test. *P* values of < 0.05 were considered to be statistically significant.

RESULTS

IFN-λ1, IFN-λ2 and IFN-λ3 demonstrate antiviral activity against HCV

To determine the antiviral effect of IL-29 (IFN-λ1), IL-28A (IFN-λ2) and IL-28B (IFN-λ3) against HCV, OR6/ORN/C-5B/KE cells were seeded in 96-well plates for 24 h and then treated with IFN-λ1, IFN-λ2, IFN-λ3 or IFN-α at various concentrations for another 24, 48 and 72 h. In this system, the *Renilla* luciferase activity reflects the amount of HCV RNA synthesized. As shown in Fig. 1, at concentrations of 1 ng/mL or more, all IFN-λs led to a concentration- and time-dependent decrease in luciferase activity of the OR6/C-5B replicon. IFN-λ3 at 10 ng/mL inhibited HCV replication (32% reduction, $P < 0.05$) to a similar extent as 0.01 ng/mL IFN-α (49% reduction, $P < 0.05$) by 48 h.

We also assessed the effects of IFN-λ1, IFN-λ2 and IFN-λ3 on Huh7.5.1/JFH-1 cells. JFH-1 cells were seeded in 96-well plates for 24 h and then treated with IFN-λ1, IFN-λ2, IFN-λ3 or IFN-α at various doses for another 48 h. To determine their antiviral effect, HCV core protein in the medium and intracellular HCV RNA were measured by CLEIA and quantitative real-time RT-PCR, respectively. HCV RNA quantitative PCR assays were multiplexed for 18s ribosomal RNA to control for the amount of input RNA. As shown in Fig. 2, all IFN-λs inhibited HCV replication in JFH-1 cells in a concentration-dependent manner. Similarly, all of the IFN-λs caused suppression of HCV core protein secretion into the cell culture medium (Figure S1).

In C-5B system, there was no evident cytotoxicity below 100 ng/mL in any interferons except for IFN-λ1 (Figure S2). On the other hand, cytotoxicity was observed in lesser concentrations by those IFNs in JFH-1 system. However, as demonstrated in Fig. 2 and Figure S3, antiviral effect exceeded the cytotoxicity in the JFH-1 system.

Synergistic inhibition of HCV replication by IFN-λ3 and IFN-α in combination

We examined whether the combination of IFN-λ3 and IFN-α induces greater antiviral activity as compared with the individual cytokines alone. OR6/ORN/C-5B/KE cells were treated with the combinations of IFN-λ3 and IFN-α at various concentrations for 48 h. As shown in Fig. 3a, the relative concentration–inhibition curves of IFN-α were plotted for each fixed concentration of IFN-λ3, and the curves shifted to the left with increasing concentrations of IFN-λ3. The results indicate a synergistic effect of IFN-λ3 and IFN-α against HCV replication. We confirmed the synergistic effect of IFN-λ3 and IFN-α by isobologram (Fig. 3b). The inhibitory effects of the combination were quantified according to the method of Chou *et al.* using the CalcuSyn software program (Biosoft, Cambridge, UK). At the ED_{50} of each drug, the combination index was 0.40-0.61, indicating significant synergism. We also assessed the effect of the combination on Huh7.5/JFH-1 cells by HCV RNA quantitative PCR assays and HCV core protein secretion. At the ED_{50} of each drug, the combination index was 0.55 and 0.48, respectively (Table S1). The cytotoxicity was not observed at the range of concentration tested (Fig. S2E, S3E).

IFN-λ3 induces ISRE promoter activity

We used the ISRE luciferase reporter assay to assess activity downstream of the JAK-STAT signalling pathway. The ISRE-firefly luciferase plasmid was transfected into OR6/ORN/C-5B/KE cells for 24 h, and these cells were cultured with various concentrations of IFN-λ3 and IFN-α for another 12, 24 or 48 h. Firefly and *Renilla* luciferase activity was then measured.

IFN-λ3 induced ISRE luciferase activity in a time-dependent manner; activity was elevated threefold after treatment with 100 ng/mL IFN-λ3 for 48 h (Fig. 4). In contrast, IFN-α induced ISRE luciferase more rapidly, producing maximal activation of the response to IFN-α at 12 h. The combination of IFN-λ3 and IFN-α induced ISRE luciferase activity similarly to IFN-λ3 alone.

IFN-α and IFN-λ3 induce expression of similar genes in HCV 1b replicon cells

OR6/ORN/C-5B/KE cells were stimulated for 6, 12, 24 and 48 h with 0.01 ng/mL IFN-α, 10 ng/mL IFN-λ3 or a combination of both, while controls were left unstimulated for the same time interval. Induction of gene expression by IFNs was analysed in microarray experiments.

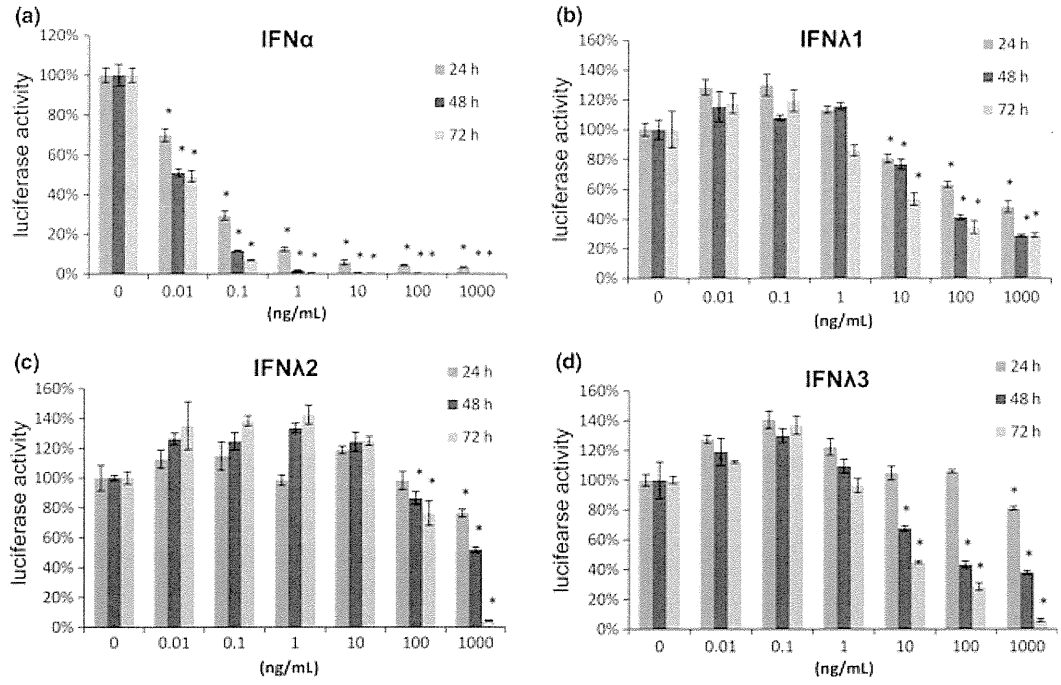

Fig. 1 IFN-α and IFN-λs inhibit HCV replicon in OR6 cells. Specific inhibition of the replication of a full-length HCV genotype 1b replicon by (a) IFN-α and (b) IFN-λ1, (c) IFN-λ2, (d) IFN-λ3 were quantified on the basis of luciferase activity. Symbols show the mean value of triplicate wells; error bars show the SD. *: $P < 0.05$ *vs* control (IFN 0 ng/mL) of each time point.

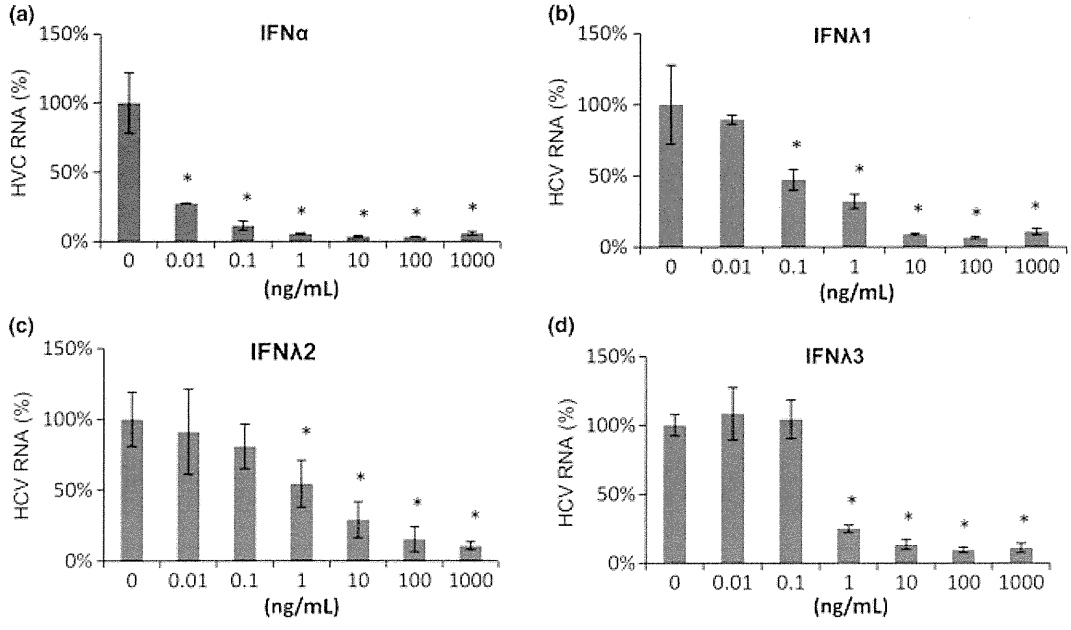

Fig. 2 IFN-α and IFN-λs inhibit HCV replicon in Huh7.5.1 cells. JFH1-infected Huh7.5.1 cells were incubated with various concentrations of (a) IFN-α and (b) IFN-λ1, (c) IFN-λ2, (d) IFN-λ3. After 48 h of treatment, total RNA was isolated and reverse transcribed, after which quantitative PCR was performed. Symbols show the mean value of triplicate wells; error bars show the SD. *: $P < 0.05$ *vs* control (IFN 0 ng/mL).

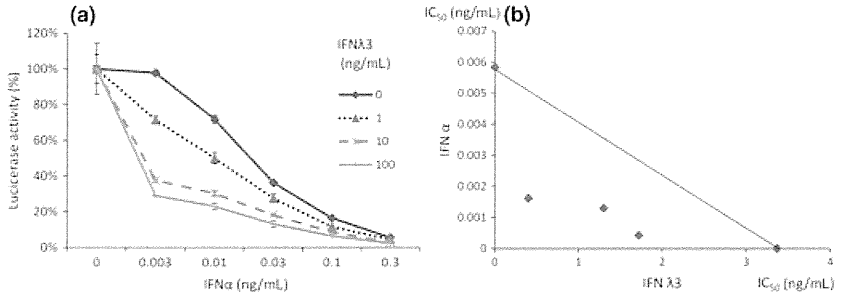

Fig. 3 Synergistic inhibitory effect of IFN-λ3 with IFN-α on hepatitis C virus replication. OR6/ORN/C-5B/KE cells were treated with combinations of IFN-λ3 with IFN-α at various concentrations. (a) The relative concentration–inhibition curves of IFN-α plotted for each fixed concentration of IFN-λ3 (0, 1, 10 and 100 ng/mL). (b) Classic isobologram for IC_{50} of IFN-λ3 with IFN-α in combination.

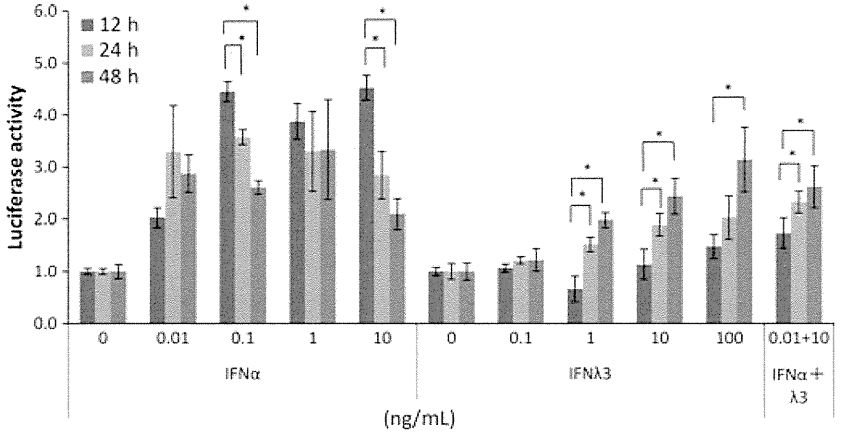

Fig. 4 IFN-stimulated response element (ISRE) promoter activity induced by IFN-α, IFN-λ3 or combination of IFN-α and IFN-λ3. OR6/ORN/C-5B/KE cells transfected with ISRE-firefly luciferase were cultured with various concentrations of IFN-α alone, IFN-λ3 alone or 0.01 ng/mL IFN-α plus 10 ng/mL IFN-λ3. ISRE-firefly luciferase activity at 24 h after transfection. Symbols show the mean value of triplicate wells; error bars show the SD. *: $P < 0.05$.

At all time points, the IFN-λ3-treated samples showed a tendency for the induction of a larger number of genes than samples treated with IFN-α. However, as shown in Table 1 listing the top 25 genes that were upregulated by both IFN-α and IFN-λ3 at 12 h, most of the upregulated genes are previously identified ISGs and the genes with high ranks were similar irrespective of the type of IFN or time point.

The time course of ISGs regulation differs between IFN-α and IFN-λ3

By microarray analysis, ISGs were more rapidly induced after the addition of IFN-α *vs* IFN-λ3 (data not shown). To confirm the rapid induction of ISGs by IFN-α, six ISGs, that is, IFI-6, IFIT1 (ISG56), DDX60, OAS2, Mx1 and USP18, were quantified for time-dependent expressional change by real-time RT-PCR. Expression of most of the genes upregulated by IFN-α peaked at 12 h and fell thereafter. In contrast, expression of IFN-λ3-induced genes peaked at 24 h and lasted up to 48 h. Combination of IFN-α and IFN-λ3 induced ISG with peak effects occurring at 12–24 h and lasting up to 48 h (Fig. 5).

DISCUSSION

In this study, we demonstrated that IFN-λ family members have distinctive time-dependent antiviral activities in an HCV replicon system and that IFN-λ3 and IFN-α have a synergistic effect in combination. Moreover, we attempted to identify the antiviral mechanism of IFN-λ3 by conducting a cDNA microarray analysis.

In previous studies, anti-HCV activity of IFN-λ1, IFN-λ2 and IFN-λ3 was reported in JFH-1 and OR6/C-5B systems [13]. Time-dependent anti-HCV activity has also been observed with IFN-λ1 [9]. In this study, we confirmed the previous results and added the further finding that time-dependent antiviral activity is not limited to IFN-λ1, but rather is common among all IFN-λs.

Table 1 Top 25 genes that were upregulated by both IFN-α and IFN-λ3 at 12 h

Gene bank ID	Gene symbol	Gene description	IFN-α 0.01 ng/mL fold increase	IFN-λ3 10 ng/mL fold increase	IFN-α+IFN-λ3 fold increase
BC007091	IFIT1	Interferon-induced protein with tetratricopeptide repeats 1	4.01	4.49	4.87
BC049215	OAS2	2′-5′-oligoadenylate synthetase 2, 69/71kDa	3.06	3.88	4.48
M33882	MX1	Myxovirus (influenza virus) resistance 1	3.24	3.29	3.69
AF095844	IFIH1	Interferon induced with helicase C domain 1	2.73	3.02	3.54
BC038115	DDX60	DEAD (Asp-Glu-Ala-Asp) box polypeptide 60	2.70	2.92	3.51
BC011601	IFI6	Interferon, alpha-inducible protein 6	3.07	3.24	3.42
BC042047	HERC6	Hect domain and RLD 6	2.56	2.75	3.34
AF442151	RSAD2	Radical S-adenosyl methionine domain containing 2	1.32	2.59	3.28
U34605	IFIT5	Interferon-induced protein with tetratricopeptide repeats 5	2.47	2.91	3.25
AY730627	OAS1	2′,5′-oligoadenylate synthetase 1, 40/46kDa	2.32	2.57	3.05
AB006746	PLSCR1	Phospholipid scramblase 1	2.37	2.51	3.03
AF307338	PARP9	Poly (ADP-ribose) polymerase family, member 9	2.39	2.46	2.94
M87503	IRF9	Interferon regulatory factor 9	2.61	2.59	2.85
AK297137	IFIT3	Interferon-induced protein with tetratricopeptide repeats 3	1.90	2.36	2.79
AK290655	EIF2AK2	Eukaryotic translation initiation factor 2-alpha kinase 2	2.47	2.45	2.77
BX648758	PARP14	Poly (ADP-ribose) polymerase family, member 14	2.07	2.25	2.66
BC132786	DDX58	DEAD (Asp-Glu-Ala-Asp) box polypeptide 58	1.83	2.17	2.59
AF445355	SAMD9	Sterile alpha motif domain containing 9	2.07	2.08	2.56
	DDX60L	DEAD (Asp-Glu-Ala-Asp) box polypeptide 60-like	1.63	1.92	2.39
BC014896	USP18| USP41	Ubiquitin-specific peptidase 18/ubiquitin-specific peptidase 41	1.52	1.78	2.11
AB044545	OAS3	2′-5′-oligoadenylate synthetase 3, 100kDa	1.44	1.57	2.10
BC010954	CXCL10	Chemokine (C-X-C motif) ligand 10	0.76	1.66	1.99
BC014896	USP18	Ubiquitin-specific peptidase 18	1.33	1.55	1.99
AL832618	IFI44L	Interferon-induced protein 44-like	0.58	1.31	1.95

We also assessed whether IFN-λ3 and IFN-α in combination could produce additive or synergistic effects on antiviral activity. In previous studies, additive antiviral activity against HCV was reported with the combination of IFN-λ1 and IFN-α [9, 10]. However, there have been no previous reports on the combined effects of IFN-λ3 and IFN-α. In this study, the focus was on IFN-λ3, because IFN-λ3 is suspected to be the key molecule, mediating the effect of SNPs in the IL-28B gene region on the anti-HCV response to IFN-α. As shown in Fig. 3 and Table S1, synergistic induction of anti-HCV activity occurred in both the OR6/C-5B and Huh7.5/JFH-1 HCV replicon systems. Synergy was demonstrated by the combination index values (Table S1).

Although it has been reported that the upregulated genes induced by IFN-λ are similar to those induced by IFN-α [9, 14–16], there have been no previous reports on

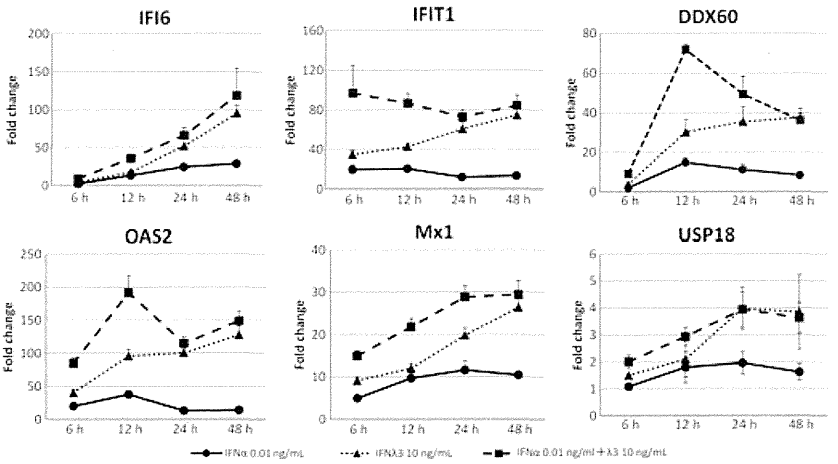

Fig. 5 Time course of ISG expression induced by 0.01 ng/mL IFN-α, 10 ng/mL IFN-λ3 or 0.01 ng/mL IFN-α plus 10 ng/mL IFN-λ3. Expression of the ISGs – IFI-6, IFIT1 (ISG56), DDX60, OAS2, Mx1 and USP18 – in OR6/ORN/C-5B/KE cells treated 6, 12, 24 and 48 h were determined by qRT-PCR. Results are presented as the relative fold induction. Symbols show the mean value of triplicate wells; error bars show the SD. *Solid lines* represent 0.01 ng/mL IFN-α alone, whereas *fine dashed lines* show 10 ng/mL IFN-λ3 alone, and *coarse dashed lines* show the combination of the 2 cytokines.

the genes induced by IFN-α and IFN-λ in combination. In cDNA microarray analysis, as demonstrated in Table 1, the most strongly upregulated genes induced by IFN-α/IFN-λ3 alone or in combination were almost identical, and most of them were ISGs. As no genes showed upregulation specific to IFN-λ3, we speculate that IFN-α and IFN-λ3 share a similar antiviral intracellular mechanism at the molecular level.

Unexpectedly in microarray analyses, synergistic upregulation of ISGs was not observed. In the same manner, TaqMan real-time RT-PCR analysis showed that the combination of IFN-α and IFN-λ3 did not upregulate ISGs synergistically (Fig. 5). In addition to cDNA microarray analysis, ISRE reporter assays were performed to determine the activation of components of the JAK-STAT pathway common to both type I and III IFNs. As shown in Fig. 4, each IFN upregulated ISRE activity, and the combination of IFN-λ3 and IFN-α did not synergistically enhance ISRE activity either.

Meanwhile, the peak time of the induction of ISG expression differs for IFN-α and IFN-λ1 [9, 17]; peak gene expression occurs earlier with IFN-α than with IFN-λ1. In our study, we confirmed that the peak induction of gene expression occurred later (24 h) and lasted longer (24–48 h) with IFN-λ3 than with IFN-α (12 h). Importantly, gene expression appeared early (12 h) and was prolonged (48 h) by the combination of both IFNs. Similarly to the peak time difference between IFN-α and IFN-λ3 seem for ISG expression, a time-dependent increase in ISRE activation was observed with the combination of both IFNs. While the precise mechanism remains to be clarified, differential regulation of the time-dependent induction of ISG gene expression could be one of the mechanisms underlying the synergistic antiviral effect. One of the molecules contributing to time-dependent ISG upregulation is the ISG known as ubiquitin-specific peptidase 18 (USP18), which has been reported to bind to IFNAR2 and inhibit the interaction of Jak1 with its receptor, thereby preventing IFN-α signalling while leaving IFN-λ signalling unaffected [18, 19]. Actually, expression of USP18 is specifically upregulated with IFN-λ3 in this study as shown in Fig. 5. If the ISGs upregulated by IFN-α are downregulated by USP18, it is plausible that the expression of genes induced by IFN-α decreases early, while expression of genes induced by IFN-λ lasts longer.

A number of clinical studies have confirmed that SNPs around the IL-28B gene are associated with the response to PEG-IFN and RBV therapy, and as previously indicated, various investigations have been performed to clarify the underlying mechanism. Specifically, increased IL-28B mRNA expression in PBMC [2, 3], high serum concentrations of IFN-λ1 (IL-29) [20], low expression of ISGs in the liver prior to IFN treatment [8, 21] and high upregulation of ISG expression by IFN treatment [8, 22] were found in subjects with IL-28B SNP genotypes associated with SVR (rs12979860 CC and rs8099917 TT). Although the functional role of IFN-λ3 still needs to be investigated more thoroughly, if IFN-λ3 expression change is the essential difference in determining the clinical treatment response to PEG-IFN and RBV therapy and if its expression is decreased in patients with the specific IL-28B genotype, which is associated with non-SVR, it is possible that exogenous administration of IFN-λ3 might improve IFN-α-induced viral clearance and that such treatment would be beneficial for patients with the IFN-resistant IL-28B genotype.

In present study, the OR6-cultured cells harboured the rs8099917 TT genotype, and recombinant IFN-λ3 (IL-

28B) protein used in the experiment was derived from cells with the rs8099917 TT genotype (data not shown). Therefore, the viral responses and/or cellular gene expression change in cells and/or proteins with different IL-28B genotypes *in vitro* should be determined in future studies.

In conclusion, we demonstrated that IFN-α and IFN-λ3 synergistically enhance anti-HCV activity *in vitro*. Although the ISGs upregulated by IFN-α and IFN-λ3 were similar, differences in time-dependent upregulation of these genes, especially prolonged ISGs expression by IFN-λ3, might contribute to their synergistic antiviral activity.

ACKNOWLEDGEMENTS

We are grateful to Ms. Sakamoto, Ms. Endo and Mr. Osada, laboratory technicians at University of Yamanashi Hospital, for quantification of HCV core protein in culture supernatant. This study was supported in part by a grant-in-aid scientific research fund of the Ministry of Education, Science, Sports and Culture number 21590836, 21590837, 23390195 and in part by a grant-in-aid from the Ministry of Health, Labour and Welfare of Japan (H22-kanen-006).

CONFLICT OF INTEREST

Shinya Maekawa and Taisuke Inoue belong to a donation-funded department that is funded by MSD co. ltd.

REFERENCES

1 Ge D, Fellay J, Thompson AJ, *et al.* Genetic variation in IL28B predicts hepatitis C treatment-induced viral clearance. *Nature* 2009; 461: 399–401.
2 Tanaka Y, Nishida N, Sugiyama M, *et al.* Genome-wide association of IL28B with response to pegylated interferon-alpha and ribavirin therapy for chronic hepatitis C. *Nat Genet* 2009; 41: 1105–1109.
3 Suppiah V, Moldovan M, Ahlenstiel G, *et al.* IL28B is associated with response to chronic hepatitis C interferon-alpha and ribavirin therapy. *Nat Genet* 2009; 41: 1100–1104.
4 Thomas DL, Thio CL, Martin MP, *et al.* Genetic variation in IL28B and spontaneous clearance of hepatitis C virus. *Nature* 2009; 461: 798–801.
5 Rauch A, Kutalik Z, Descombes P, *et al.* Genetic variation in IL28B is associated with chronic hepatitis C and treatment failure: a genome-wide association study. *Gastroenterology* 2010; 138:1338–1345, 1345 e1331-1337.
6 Dellgren C, Gad HH, Hamming OJ, Melchjorsen J, Hartmann R. Human interferon-lambda3 is a potent member of the type III interferon family. *Genes Immun* 2009; 10: 125–131.
7 Kotenko SV, Gallagher G, Baurin VV, *et al.* IFN-lambdas mediate antiviral protection through a distinct class II cytokine receptor complex. *Nat Immunol* 2003; 4: 69–77.
8 Honda M, Sakai A, Yamashita T, *et al.* Hepatic ISG expression is associated with genetic variation in interleukin 28B and the outcome of IFN therapy for chronic hepatitis C. *Gastroenterology* 2010; 139: 499–509.
9 Marcello T, Grakoui A, Barba-Spaeth G, *et al.* Interferons alpha and lambda inhibit hepatitis C virus replication with distinct signal transduction and gene regulation kinetics. *Gastroenterology* 2006; 131: 1887–1898.
10 Pagliaccetti NE, Eduardo R, Kleinstein SH, Mu XJ, Bandi P, Robek MD. Interleukin-29 functions cooperatively with interferon to induce antiviral gene expression and inhibit hepatitis C virus replication. *J Biol Chem* 2008; 283: 30079–30089.
11 Ikeda M, Abe K, Dansako H, Nakamura T, Naka K, Kato N. Efficient replication of a full-length hepatitis C virus genome, strain O, in cell culture, and development of a luciferase reporter system. *Biochem Biophys Res Commun* 2005; 329: 1350–1359.
12 Aoyagi K, Ohue C, Iida K, *et al.* Development of a simple and highly sensitive enzyme immunoassay for hepatitis C virus core antigen. *J Clin Microbiol* 1999; 37: 1802–1808.
13 Zhang L, Jilg N, Shao RX, *et al.* IL28B inhibits hepatitis C virus replication through the JAK-STAT pathway. *J Hepatol* 2011; 55: 289–298.
14 Ank N, West H, Bartholdy C, Eriksson K, Thomsen AR, Paludan SR. Lambda interferon (IFN-lambda), a type III IFN, is induced by viruses and IFNs and displays potent antiviral activity against select virus infections in vivo. *J Virol* 2006; 80: 4501–4509.
15 Zhou Z, Hamming OJ, Ank N, Paludan SR, Nielsen AL, Hartmann R. Type III interferon (IFN) induces a type I IFN-like response in a restricted subset of cells through signaling pathways involving both the Jak-STAT pathway and the mitogen-activated protein kinases. *J Virol* 2007; 81: 7749–7758.
16 Doyle SE, Schreckhise H, Khuu-Duong K, *et al.* Interleukin-29 uses a type 1 interferon-like program to promote antiviral responses in human hepatocytes. *Hepatology* 2006; 44: 896–906.
17 Maher SG, Sheikh F, Scarzello AJ, *et al.* IFNalpha and IFNlambda differ in their antiproliferative effects and duration of JAK/STAT signaling activity. *Cancer Biol Ther* 2008; 7: 1109–1115.
18 Makowska Z, Duong FH, Trincucci G, Tough DF, Heim MH. Interferon-beta and interferon-lambda signaling is not affected by interferon-induced refractoriness to interferon-alpha in vivo. *Hepatology* 2011; 53: 1154–1163.
19 Franois-Newton V, de Freitas Almeida GM, Payelle-Brogard B, *et al.*

USP18-Based Negative Feedback Control Is Induced by Type I and Type III Interferons and Specifically Inactivates Interferon α Response. *PLoS ONE* 2011; 6: e22200.
20 Langhans B, Kupfer B, Braunschweiger I, *et al.* Interferon-lambda serum levels in hepatitis C. *J Hepatol* 2011; 54: 859–865.
21 Urban TJ, Thompson AJ, Bradrick SS, *et al.* IL28B genotype is associated with differential expression of intrahepatic interferon-stimulated genes in patients with chronic hepatitis C. *Hepatology* 2010; 52: 1888–1896.
22 Abe H, Hayes CN, Ochi H, *et al.* IL28 variation affects expression of interferon stimulated genes and peg-interferon and ribavirin therapy. *J Hepatol* 2011; 54: 1094–1101.

SUPPORTING INFORMATION

Additional Supporting Information may be found in the online version of this article:

Figure S1: IFN-α and IFN-λs inhibit HCV core protein secretion. JFH1-infected Huh7.5.1 cells were incubated with various concentrations of IFN-α and IFN-λ1, -λ2, -λ3. After 48 h of treatment, HCV core protein in the medium was measured. Symbols show the mean value of triplicate wells; error bars show the SD. *: $p < 0.05$ vs. control (IFN 0ng/ml).

Figure S2: The dimethylthiazol carboxymethoxyphenyl sulfophenyl tetrazolium assay was performed after OR6/ORN/C-5B/KE cells were cultured with various concentrations of (A) IFN-α, (B) IFN-λ1, (C) IFN-λ2, (D) IFN-λ3 and (E) combination of IFN-α and IFN-λ3 for 48 h. Symbols show the mean value of triplicate wells; error bars show the SD. *: $p < 0.05$ vs. control (IFN 0ng/ml).

Figure S3: The dimethylthiazol carboxymethoxyphenyl sulfophenyl tetrazolium assay was performed after Huh7.5.1/JFH-1 cells were cultured with various concentrations of (A) IFN-α, (B) IFN-λ1, (C) IFN-λ2, (D) IFN-λ3 and (E) combination of IFN-α and IFN-λ3 for 48 h. Symbols show the mean value of triplicate wells; error bars show the SD. *: $p < 0.05$ vs. control (IFN 0ng/ml).

Table S1: Combination index after 48hr stimulation by CalucSyn.

Please note: Wiley-Blackwell are not responsible for the content or functionality of any supporting materials supplied by the authors. Any queries (other than missing material) should be directed to the corresponding author for the article.